PREPARATION AND CHARACTERIZATION OF NATURAL FIBRE/CO-POLYESTER BIOCOMPOSITES

by

THABANG HENDRICA MOKHOTHU (B.Sc. Hons.)

Submitted in accordance with the requirements for the degree

MASTER OF SCIENCE (M.Sc.)

Department of Chemistry

Faculty of Natural and Agricultural Sciences

at the

UNIVERITY OF THE FREE STATE (QWAQWA CAMPUS)

SUPERVISOR: PROF AS LUYT
CO-SUPERVISOR: DR BR GUDURI

7 December 2010

DECLARATION

I hereby declare that the research in this thesis is my own independent work, and has not previously been submitted to any other University in order to obtain a degree. I further cede copyright of the dissertation in favour of the University of the Free State.

_____ _____

T.H. Mokhothu Prof. A.S. Luyt

DEDICATION

This work is dedicated to the entire family of Mokhothu for their love and support. To Matlholi Jerminah (mom), Constance Motlalepule (grandmother), Tshepiso (sister), a special gratitude to my new family Bokamoso Elizabeth and her mom Nthabiseng Mirriam.

"TO GOD BE THE GLORY"

ABSTRACT

The effects of natural fibre modification with sodium hydroxide, silane and Disperal nano-powder were investigated for copolyester/kenaf fibre biocomposites. The kenaf fibre was modified with sodium hydroxide followed by silane at different concentration (3, 6 and 9%). The 3% silane modified fibre was further modified with Disperal at different concentrations (4, 6, 8 and 10 wt%) as an additive. The biocomposites were prepared by a melt mixing process using a Haake Rheomix mixer. The biocomposites were characterized for their morphology, thermal properties, mechanical properties, thermomechanical properties, biodegradability and the amount of crosslinking. The properties were determined using scanning electron microscopy (SEM), differential scanning calorimetry (DSC), thermogravimetric analysis (TGA), tensile testing, dynamic mechanical analysis (DMA), biodegradability testing and gel content determination. Compatibility of the natural fibre and the copolyester (CP) matrix is necessary as morphology has a significant effect on the composite properties. The SEM images show less fibre pullout for the silane modified composites with increasing concentration. DSC results show that the silane treated composites had a slight shift in the melting temperature due to reduced chain mobility as a result crosslinking or grafting. The melting enthalpy values were too scattered to make definite conclusions on changes in the crystallinities for the silane and Disperal modified composites. The TGA results showed improved thermal stability for the NaOH treated composite compared to both the silane and Disperal modified composites. The DMA results were in line with the other thermal analysis results, and will also be discussed. The biodegradability tests confirmed the biodegradability of the systems.

LIST OF ABBREVIATIONS AND SYMBOLS

PHB	Polyhydroxybutyrate
CP	Copolyester
ASTM	American Society for Testing and Materials
DMA	Dynamic mechanical analysis
DSC	Differential scanning calorimetry
SEM	Scanning electron microscopy
TGA	Thermogravimetric analysis
FTIR	Fourier-transform infrared spectroscopy
DP	Degree of polymersization
PLAF	Pineapple leaf fibre
PLA	Poly(lactic acid)
PCL	Poly(ε-caprolactone)
PBS	Poly(butylene succinate)
PHBV	Poly(3-hydroxybutyrate-co-3-hydroxyvalerate)
PBT	Polybutylene terephthalate
AA-abaca	Acetic anhydride treated abaca fibre
PEA	Polyester amide
PS	Polystyrene
UV	Ultraviolet
FIBNA	Alkali treated fibre
FIB	Untreated fibre
FIBSI	Silane treated fibre
FIBNASI	Alkali followed by silane treated fibre
APS	3-aminopropyltriethoxysilane
CO_2	Carbon dioxide
M_n	Molecular weight
T_g	Glass transition temperature
T_m	Melting temperature
pbw	Parts by weight
rpm	Revolutions per minute
Silane A 172	Vinyltri(2-ethoxymethoxy)silane

Silane A 100	γ-aminopropyltrimethoxysilane
kGy	Kilogrey's
kGy s^{-1}	Kilogrey's per second
MPa	Megapascal
BA	Boehmite aluminium powder
T_c	Crystallization temperature
T_d	Decomposition temperature
ΔP	Power compensation
ΔT	Heat flux
ΔH_m^{obs}	Observed melting enthalpy
ΔH_m^{cal}	Calculated melting enthalpy
E'	Storage modulus
E''	Loss modulus
tan δ	Damping coefficient

TABLE OF CONTENTS

LIST OF TABLES

LIST OF FIGURES

CHAPTER ONE

INTRODUCTION

1.1 Background

Over the last decades, research has increasingly been conducted on renewable materials from sustainable resources for a variety of applications. This has been influenced by the ever-increasing demand for newer, stronger, stiffer, recyclable, fire repellent, less expensive and yet lighter-weight materials in fields such as aerospace, transportation, construction and packaging industries. Factors such as increased environmental and health concerns, a need for waste management solutions, more sustainable methods of manufacturing and reduced energy consumption, are reasons for the need to replace conventional composites (glass, carbon and synthetic fibres). Therefore, material components such as natural fibres and biodegradable polymers can be considered as alternatives for the development of new biodegradable composites or biocomposites. [1-9].

1.2 Biocomposites from renewable resources

Biocomposites are composite materials comprising of biodegradable polymers as the matrix material and biodegradable fillers, usually biofibres (e.g. lignocellulose fibres). Natural fibres, such as cotton, flax, hemp, kenaf etc. or fibres from recycled wood or waste paper, or even by-products from food crops are examples used for the production of biocomposite materials [2]. Hence composites made with natural fibres are known as “green composites” [3].

In contrast to synthetic polymer composites, biocomposites have polymer matrices ideally derived from renewable resources such as vegetable oils or starches. Polymer matrices from renewable resources are becoming attractive alternatives, due to their abundance, availability, renewability and relatively low cost. Various biodegradable polymers have been used for the matrix such as polyesters (polyhydroxybutyrate (PHB)) or starch (polysaccharides). Incorporating biopolymers with natural fibres is a promising solution to replace conventional composites because they are environmentally friendly [1,11].

Avérous *et al*. [6] presented the classification of biodegradable polymers in different families (Figure 1.1). Except for the fourth family, which is of fossil origin, most biodegradable polymers are obtained from renewable resources (biomass). The first family are the agro-polymers (polysaccharides), obtained from biomass by fractionation. The second and third families are polyesters obtained by fermentation from biomass or from genetically modified plants, or synthesized from monomers obtained from biomass. The fourth family are polyesters that are totally synthesized through petrochemical processes from fossil resources.

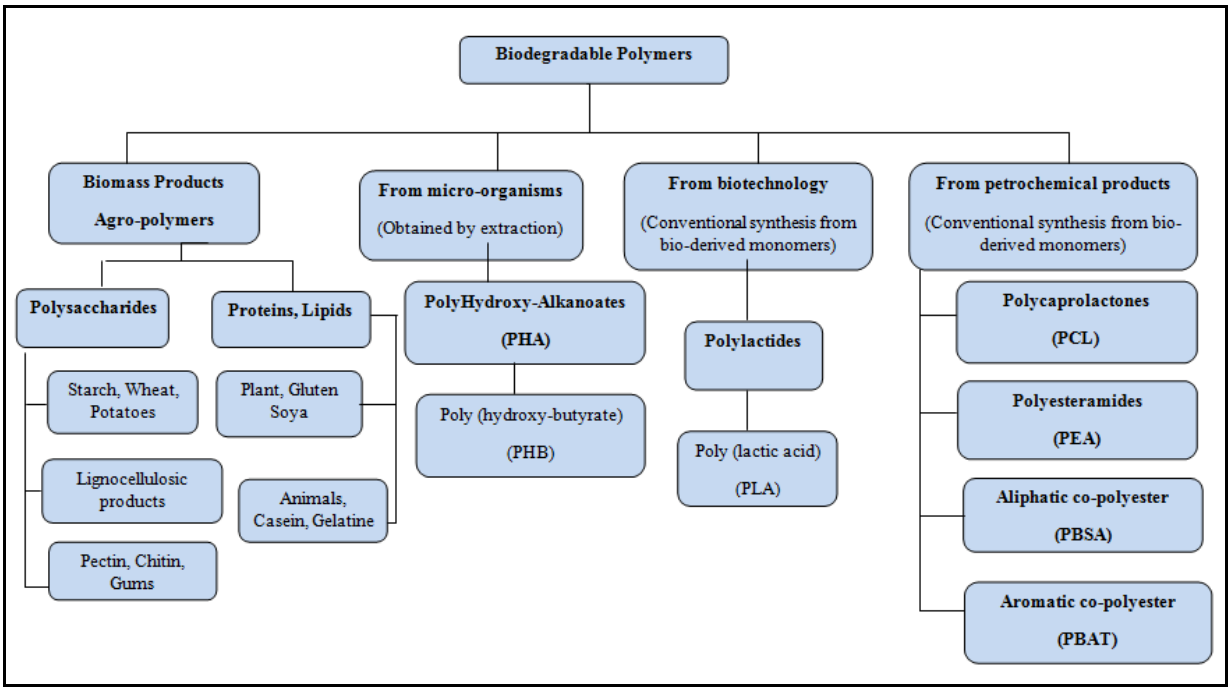

Figure 1.1 Classification of biodegradable polymers

Biodegradable matrices are available commercially in large numbers and exhibit a wide range of properties. At present they can compete with non-biodegradable matrices in different industrial fields (packaging, agricultural products and cutlery). In this wide range there also are the lignocellulose-based fibres used as biodegradable fillers (Table 1.1). These fibres have a number of significant mechanical and physical properties. These attractive properties also motivate more and more industrial sectors (e.g. structural and automotive parts, building materials) to replace commonly used glass fibre with natural fibres, because they are of low cost and composites made from them are expected to be lightweight. With their environmentally friendly character and some economical advantages, investigations of biocomposite materials have not only been a challenge to materials scientists, but their use has

also been an important provider of opportunities to improve the standard of living of people around the world [7,10].

Table 1.1 Chemical compositions (wt %) of vegetable fibres [2,11]

Fibres	Cellulose	Hemicellulose	Pectin	Lignin	Ash
Bast fibre					
Kenaf	36	21	18	0.8-2	2-5
Flax	71	19	2	2	1-2
Jute	72	13	>1	13	8
Hemp	75	13	1	4	1-2
Leaf Fibre					
Sisal	73	13	1	11	7
Abaca	70	22	1	6	1
Seed-hair Fibres					
Cotton	93	3	3	-	1
Wheat Straw	51	26	-	16	7

Biocomposites materials provide a competitive advantage over glass-reinforcement composites in many applications. They can contribute to economic improvement, such as new agricultural activities and environmental issues. Several critical issues related to biofibres are (i) surface treatment to make it a suitable reinforcing filler for composite application, (ii) their hydrophilic properties, which may affect the properties of the biocomposite material, and (iii) the development of appropriate processing techniques, depending on the type of fibre form (chopped, nonwoven/woven fabric, yarn) [2,11].

1.3 Drawbacks and advantages on the use of biocomposites

The use and production of biocomposite materials has grown extensively and has brought positive advantages for the manufacturing and industrial sectors over traditional reinforcing fibres like glass. However, the main drawback of natural fibres is that their hydrophilic property reduces their compatibility with hydrophobic polymer matrix during composite fabrication. As a result, the poor fibre-matrix adhesion causes reduced mechanical properties. Therefore, it is necessary to improve the mechanical and other properties of biocomposites by introducing chemical treatments to the natural fibres. Another disadvantage is the low

processing temperatures that must be used because of the possibility of thermal degradation of the fibre, which might affect the biocomposite properties.

Advantages of natural fibres over other reinforcing materials like glass fibre are their low cost, low density, acceptable specific strength properties, enhanced energy recovery, and biodegradability. Although these green composites are not as strong as the traditional glass fibre reinforced composites, the moderate mechanical properties are suitable for applications in non-durable consumer products and packing materials. Moreover, the hollow tubular structure of natural fibres reduces their bulk density. Therefore, biocomposites made from them are expected to be lightweight. Several studies have been conducted to improve and optimize the performance of biocomposites or biodegradable materials [2,11,12,17-21].

1.4 Applications of bio-based materials

Recent work on biocomposites reveals that in most cases the specific mechanical properties of biocomposites are comparable to widely used glass fibre reinforced plastics. Various complex structures, i.e., tubes, sandwich plates and car door interior panelling have been made from biocomposites. Starch-based materials based on recycled fibres are currently used in the packaging industry for boxes and other rigid packing media [2]. The use of natural fibres as reinforcement has grown significantly in the automotive and aerospace industries. This is due to the hollow structure of natural fibres that provides a better insulating property against noise and heat. Mostly these fibre reinforced biocomposites are used for the door or ceiling panels, and panels separating the engine and the passenger compartment. They are usually applied in formed interior parts, because these components do not need load bearing capacity, but dimensional stability is important. Biobased vehicles are lighter, making them a more economical choice for consumers. They reduce fuel cost. They exhibit a favourable nonbrittle fracture on impact, which is an important requirement in the passenger compartment. In addition to the components for the interior design of motor vehicles, panelling in railway carts or aircrafts realized so far, and therefore it is also important for these composites to be flame resistant. Therefore studies, aiming at the modification of biocomposites with flame retardants to give them good thermal properties, form part of current research activities [13-16].

1.5 Objectives

The overall objective of this study was to investigate the thermal and reinforcement properties of modified natural fibre (kenaf) introduced into a copolyester biomatrix ((aliphatic-aromatic copolyester (CP) (trade-name Ecoflex)). The natural fibre was modified by alkaline treatment, followed by silane coupling. The reasons for applying alkaline treatment on the fibre surface was: (i) to distribute the hydrogen bonds in the network structure, thereby increasing the surface roughness, (ii) to remove a certain amount of lignin, wax and natural oils covering the external surface of the fibre wall, and (iii) to depolymerize and expose the short length crystallites. Boehmite aluminium powder (Disperal nano-powder) was used to improve the thermal stability of the resulting biocomposites. The samples were characterized using scanning electron microscopy (SEM), thermogravimetric analysis (TGA), differential scanning calorimetry (DSC), tensile testing, dynamic mechanical analysis (DMA), biodegradability testing, Fourier transform infrared spectroscopy (FTIR) and gel content analysis (to determine the extent of crosslinking or grafting in the composites).

1.6 Thesis outline

The outline of this thesis is as follows

Chapter 1: Background and objectives

Chapter 2: Literature survey

Chapter 3: Experimental

Chapter 4: Results and discussion

Chapter 5: Conclusions

1.7 References

1. W. Liu, A.K. Mohanty, L.T. Drzal, M. Misra. Novel biocomposites from native grass and soy based bioplastic: Processing and properties evaluation. Industrial & Engineering Chemistry Research 2005; 44:7105-7112.
   DOI: 10.102/ie050257
2. P.A. Fowler, J.M. Hughes, R.M. Elias. Biocomposites: technology, environmental credentials and market forces. Journal of the Science of Food and Agriculture 2006; 86:1781-1789.

DOI: 10.1002/jsfa.2558

3. B.R. Guduri, A.V. Rajulu, A.S. Luyt. Effects of alkali treatment on the flexural properties of *Hildegardia* fabric composites. Journal of Applied Polymer Science 2006; 102:1297-1302.
DOI: 10.1002/app.23522

4. K. Badri, K. Anuar Mat Amin. Biocomposites from oil palm resources. Journal of Oil Palm Research 2006; Special Issue: 103-113.
DOI:

5. A. Le Duigou, I. Pilin, A. Bourmaud, P. Davies, C. Baley. Effects of recycling on mechanical behavior of biocompostable flax/poly(L-lactide) composites. Composites Part A 2008; 39:1471-1478.
DOI: 10.1016/j.compositesa.2008.05.008

6. L. Avérous, N. Boquillon. Biocomposites based on plasticized starch: thermal and mechanical behaviours. Carbohydrate Polymers 2004; 56:111-122.
DOI: 10.1016/j.carbpol.2003.11.015

7. L. Avérous, F. Le Digabel. Properties of biocomposites based on lignocellulosic fillers. Carbohydrate Polymers 2006; 66:480-493.
DOI: 10.1016/j.carbpol.2006.04.004

8. G. Mehta, A.K. Mohanty, M. Misra, L.T. Drzal. Biobased resin as a toughening agent for biocomposites. Green Chemistry 2004; 6:254-258.
DOI: 10.1039/b316658a

9. J. Nickel, U. Riedel. Activities in biocomposites. Materials Today 2003; 6:44-48.

10. A.K. Mohanty, M. Misra, L.T. Drzal. Sustainable bio-composites from renewable resources: Opportunities and challenges in the green material world. Journal of Polymers and the Environment 2002; 10:19-26.
DOI: 10.1023/A.1021013921916

11. J. Biagiotti, D. Puglia, J. M. Kenny. A review on natural fibre-based composites Part I: Structure, processing and properties of vegetable fibres. Journal of Natural Fibres 2004; 1:37-67.
DOI: 10.1300/J395v01n02_04

12. A. Arbelaiz, B. Fernández, J.A. Romas, A. Retegi, R. Llano-Ponte, I. Mondragon. Mechanical properties of short fibre bundle/polypropylene composites: Influence of matrix/fibre modification, fibre content, water uptake and recycling. Composites Science and Technology 2005; 65:1582-1592.

DOI: 10.1016/j.compscitech.2005.01.008

13. A.K. Mohanty, M. Misra, G. Hinrichsen. Biofibres, biodegradable polymers and biocomposites: An overview. Macromolecular Materials and Engineering 2000; 276-277:1-24.
DOI: 10.1002/(SICI)1439-2054(20000301)

14. R. Kozlowski, M. Wladyka-Przybylak. Flammability and fire resistance of composites reinforced by natural fibers. Polymers for Advanced Technology 2008; 19:446-453.
DOI: 10.1002/part.1135

15. A.S. Herrmann, J. Nickel, U. Riedel. Construction materials based upon biological renewable resources – from components to finished parts. Polymer Degradation and Stability 1998; 59:251-261.
DOI: 10.1016/S0141-3916(97)00169-9

16. U. Riedel. Natural fibre-reinforced biopolymers as construction materials – new discoveries. 2nd International Wood and Natural Fibre Composites Symposium, Kassel, Germany. 28-29 June 1999.

17. X. Li, L.G. Tabil, S. Panigrahi. Chemical treatments of natural fiber for use in natural fiber-reinforced composites: a review. Journal of Polymers and the Environment 2007; 15: 25-33.
DOI: 10.1007/s10924-006-0042-3

18. R. Agrawa, N.S. Saxena, K.B. Sharma, S. Thomas, M.S. Sreekala. Activation energy and crystallization kinetics of untreated and treated oil palm fibre reinforced phenol formaldehyde composites. Materials Science and Engineering 2000; 277: 77-82.
DOI: 10.1016/S0921-5093(99)00556-0

19 M. Jacob John, R.D. Anandjiwana. Chemical modification of flax reinforced polypropylene composites. Composites Part A 2009; 40:442-448.
DOI: 10.1016/j.compositesa.2009.01.007

20. W.L. Lai, M. Mariatti, J.S. Mohamad. The properties of woven kenaf and betel palm (*Areca catechu)* reinforced unsaturated polyester composites. Polymer-Plastics Technology and Engineering 2008; 47:1193-1199.
DOI: 10.1080/03602550802392035

21. V.M Khumalo, J. Karger-Kocsis, R. Thomann. Polyethylene/synthetic boehmite alumina nanocomposites: structure, thermal and rheological properties. eXPRESS Polymer Letters 2010; 4:264-274.
DOI: 10.3144/expresspolymlett.2010.34

CHAPTER TWO

LITERATURE SURVEY

2.1 Introduction

The incorporation of natural fibres into biodegradable polymers has been a subject of interest in many research fields. This is brought about by their ability to replace conventional composites and to be easily disposed from the environment. The primary purpose of making these materials is that superior or important properties compared to that of the individual components can be achieved. Natural fibre reinforced copolyester biocomposites show interesting properties due improved in compatibility between the filler and the matrix. The research work done on biocomposites is mostly on the comparison of untreated and treated fibre composites [1-16]. The most important aspects from this research work will be summarized in the remainder of this chapter.

2.2 Natural fibres

2.2.1 Structure and properties of natural fibres

In recent years polymer composites containing natural fibres have received considerable attention both in literature and in industry. The growing interest in using natural fibres as a reinforcement of polymeric based composites is mainly due to their abundant, renewable origin, relatively high specific strength and modulus, light weight, inexpensiveness and biodegradability [17-23]. Over the past decade natural fibres has found use as a potential resource for making low-cost composite material, mostly in tropical countries where these fibres are abundant [24-27]. A better understanding of chemical composition and surface adhesive bonding of natural fibres is necessary for developing natural fibre reinforced composites. Natural fibre consists of cellulose, hemicellulose, lignin, pectin, fat, wax and water soluble substances. These compositions may differ with test methods and with growing conditions even for the same kind of fibre [28-30].

Cellulose is the primary component of natural fibres. It is a linear condensation polymer consisting of D-anhydro-glucopyranose units joined together by β-1,4–glucosidic bonds. The

glucose is bonded to the next glucose through 1 and 4 carbons (Figure 2.1) to form celloboise. The overall structure of cellulose consists of crystalline and amorphous regions. The mechanical properties of the natural fibres are dependent on the cellulose content in the fibre, the degree of polymerization of the cellulose and the microfibril angle [23,31,32].

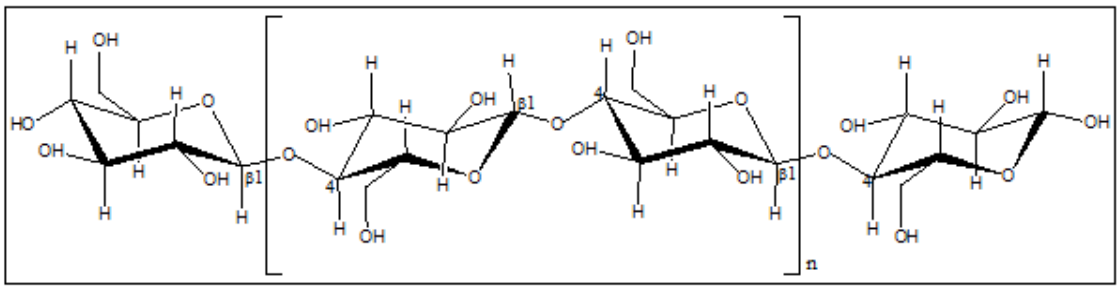

Figure 2.1 Molecular structure of cellulose

Hemicelluloses are polysaccharides and differ from cellulose in that they consist of several sugar moieties, which are mostly branched, and have a significantly lower molecular weight with a degree of polymersization (DP) of 50-200. These sugars include glucose but also other monomers such as galactose, mannose, xylose and arabinose (Figure 2.2). Hemicellulose is partly soluble in water and hydroscopic because of its open structure which contains hydroxyl and acetyl groups [31,32].

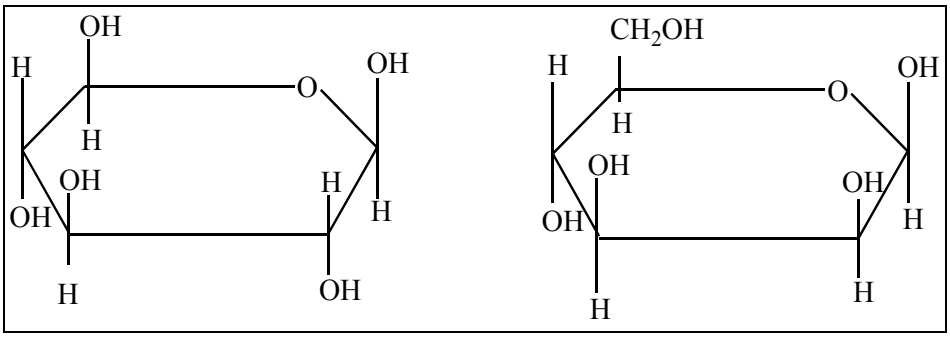

Figure 2.2 Examples of two hemicellulose sugar monomers

Lignin is a randomly branched polyphenol, made up of phenylpropane (C9) units and it is the most complex polymer among naturally occurring high-molecular-weight materials. Due to its lipophilic character, lignin decreases the permeation of water across the cell walls, which consist of cellulose fibres and amorphous hemicelluloses, and thereby assists the transport of aqueous solutions of nutrients and metabolites in the conducting xylem tissue. Lignin imparts

rigidity to the cell walls and functions together with hemicelluloses to bind cells in wood parts of plants, generating a composite structure with outstanding strength and elasticity. However, lignified materials effectively resist attacks by microorganisms by impeding penetration of destructive enzymes into the cell walls [31,32].

The lignocellulosic fibres are degraded biologically because of organisms that can recognise the carbohydrate polymers, mainly hemicellulose in the cell wall. They have very specific enzyme systems capable of hydrolysing these polymers into digestible units. The degradation process depends on how the lignocellulosic components interact in different degradation conditions (Table 2.1). Biodegradation of the high molecular weight cellulose weakens the lignocellulosic cell wall because crystalline cellulose is primarily responsible for the strength of the lignocellulosic [31].

Table 2.1 Degradation processes of natural fibres

Biological degradation	**Moisture absorption**
Hemicellulose	Hemicellulose
Non-crystalline cellulose	Non-crystalline cellulose
Crystalline cellulose	Lignin
Lignin	Crystalline cellulose
Thermal degradation	**Ultraviolet degradation**
Hemicellulose	Lignin
Cellulose	Hemicellulose
Lignin	Non-crystalline cellulose
	Crystalline cellulose
Strength	
Crystalline cellulose	
Non-crystalline cellulose	
Hemicellulose	
Lignin	

Natural fibres are a class of hair-like materials that are continuous filaments or are in discrete elongated pieces, similar to pieces of thread. They can be spun into filaments, thread or rope. They can be used as components of composites materials. Natural fibres obtained from the various parts of the plants are known as ‘plant fibres’, ‘cellulose fibres’ or ‘vegetable fibres’.

They can be classified according to which part of the plant they are obtained from (Figure 2.3). The most widely used vegetable fibres are cotton, flax and hemp, although sisal, jute, kenaf, bamboo and coconut are also widely used.

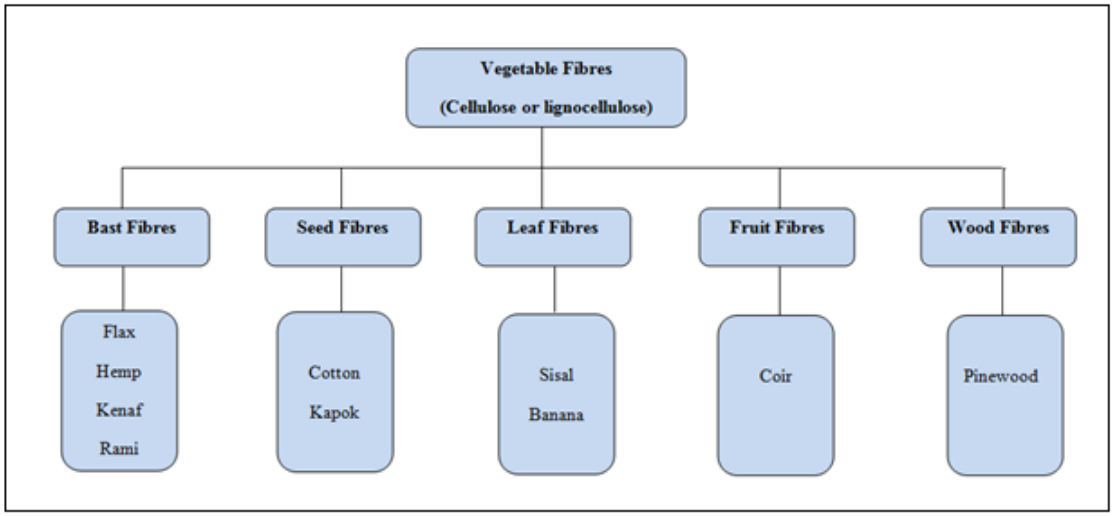

Figure 2.3 Classification of vegetable fibres

Natural fibres possess desirable properties such as high specific strength, ease of separation, enhanced energy recovery, high toughness, a non-corrosive nature, low density, low cost, good thermal properties, and biodegradability [31,22-25]. However, the majority of cellulose fibres have low degradation temperatures (~200 °C), which make them unsuitable for processing with thermoplastics above 200 °C. Their high moisture uptake and their tendency to form aggregates during processing, represent some of the drawbacks related to their use in cellulose fibre composites. The behaviour and properties of these fibres depend on many factors such as harvest period, weather variability, quality of soil, and climate of the specific geographical location [20,21]. Recent developments showed that it is possible to improve the mechanical properties of cellulose fibre-reinforced composites by chemical modification that may promote good adhesion between the polymer and the fibres.

2.2.2 Natural fibre surface modification

Natural fibres are considered as potential replacements for man-made fibres in composite materials. Although natural fibres have advantages of being low cost and low density, they are not totally free of problems. A serious problem of natural fibres is their strong polar character

which creates incompatibility with most polymer matrices. Surface treatments, although having a negative impact on economics, are potentially able to overcome the problem of incompatibility. Chemical treatments can increase the interfacial adhesion between the fibre and matrix, and decrease the water absorption of fibres, and can be considered in modifying the properties of natural fibres. Some compounds are known to promote adhesion by chemically coupling the adhesive to the material, such as sodium hydroxide, silane, acetic acid, acrylic acid, maleated coupling agents, isocyanates, potassium permanganate, and peroxide. Chemical modifications of natural fibres aimed at improving the adhesion with a polymer matrix were investigated by a number of researchers. Most chemical treatments have achieved various levels of success in improving fibre strength, fibre fitness and fibre–matrix adhesion in natural fibre-reinforced composites [31,33].

2.2.2.1 Alkaline treatment

Alkaline treatment or mercerization is one of the most used chemical treatments of natural fibres when used to reinforce thermoplastics and thermosets. The important modification done by alkaline treatment is the distribution of hydrogen bonding in the network structure, thereby increasing surface roughness [33].

Liu *et al.* [34] investigated the processing and properties of Indian grass fibre reinforced soy based biocomposites that were prepared by using twin-screw extrusion and injection molding. The Indian grass fibre was treated with an alkali solution and the other portion was used as raw. It was found that the dispersion of the raw grass fibre in the matrix was not uniform, and most of the fibres were bunched. However, the dispersion of alkali-treated grass fibre in the matrix was improved and the fibre size was reduced. The alkali-treated fibre reinforced composites also became separated fibril reinforced composites. The aspect ratio of the fibre in the matrix was improved and so was the interaction area between the fibre and the matrix. The tensile properties of 30 wt% alkali-treated grass fibre reinforced composites improved by 60%, the flexural strength by 40% and the impact strength by 30%, compared to the 30 wt% raw fibre-reinforced composites.

Edeerozey *et al.* [35] studied the surface modification of kenaf fibre by using different concentrations of NaOH (3%, 6% and 9%). The morphological and structural changes of the fibres were investigated by scanning electron microscopy (SEM). It was found that 3% NaOH

treatment was ineffective to remove the impurities on the fibre surface, while 9% NaOH treatment showed the cleanest fibre surface. The tensile strength of the kenaf fibre after treatment was measured through a fibre bundle tensile test. The fibre treated with 6% NaOH in a water bath (95°C) showed a higher unit break value than the fibre treated with 6% NaOH at room temperature. This was attributed to the effectiveness of the cleaning process of the fibre at elevated temperatures. However, when the NaOH concentration was increased to 9%, the average unit break decreased significantly. The 9% NaOH treated fibre was too strong and might have damaged the fibres, hence resulting in lower tensile strength. Lai *et al*. [36] studied the surface modification of betel palm and kenaf fibres by using 6% concentration of NaOH solution for 3 hours at room temperature. The kenaf and betel palm reinforced unsaturated polyester composites were prepared by a vacuum bagging technique. The 6% NaOH treated fibre composites showed an improvement in flexural properties compared to the untreated fibre composites. In general, the mechanical properties of the woven composites made from alkali-treated fibres were superior to those made from untreated fibres.

Ibrahim *et al.* [37] studied the effects of fibre treatment on the mechanical properties of kenaf fibre and Ecoflex (copolyester) composites. The composites were prepared using different fibre loadings and the fibre was treated with various concentrations of NaOH solution by soaking for 3 hours. Compounding of the composites was carried out at different fibre loadings (10%, 20%, 30%, 40%, and 50%) using a Brabender internal mixer. The composites were then melt-pressed to produce biodegradable kenaf/Ecoflex sheets. The results showed that 40% fibre loading generally improved the tensile strengths, and the fibre treated with 4% NaOH was found to enhance the tensile and flexural properties compared to the untreated fibre. At lower NaOH concentration the efficiency to remove impurities was not good enough. This resulted in poor bonding of the fibre to the matrix.

Sharifah *et al.* [38] studied the effects of alkalization and fibre alignment of kenaf and hemp bast fibre composites. Long and random hemp and kenaf fibres were alkalized with 6% NaOH solution. Examinations were carried out on the untreated and alkalized fibres to study the morphological changes that occurred after treatment. The SEM micrograph of the longitudinal surface of the untreated fibre bundles, for both kenaf and hemp fibres, showed the presence of wax, oil and surface impurities. In contrast to the untreated fibres, the longitudinal view of 6% NaOH treated kenaf and hemp fibres, showed a very clean surface. The surface of the treated fibres appeared to be smooth, but in fact was roughened by the chemical treatment.

2.2.2.2 Silane treatment

Silane is a chemical compound with a chemical formula SiH_4. Silanes are used as coupling agents to let natural fibres adhere to the polymer matrix, stabilizing the composite material. Silane coupling agents may reduce the number of cellulose hydroxyl groups in the fibre-matrix interface. In the presence of moisture, hydrolysable alkoxy groups lead to the formation of silanols. The silanol then reacts with the hydroxyl group of the fibre, forming stable covalent bonds to the cell wall that are chemisorbed onto the fibre surface (Figure 2.4) [39]. Therefore, the hydrocarbon chains provided by the application of silane restrain the swelling of the fibre by creating a crosslinked network due to covalent bonding between the matrix and the fibre [33].

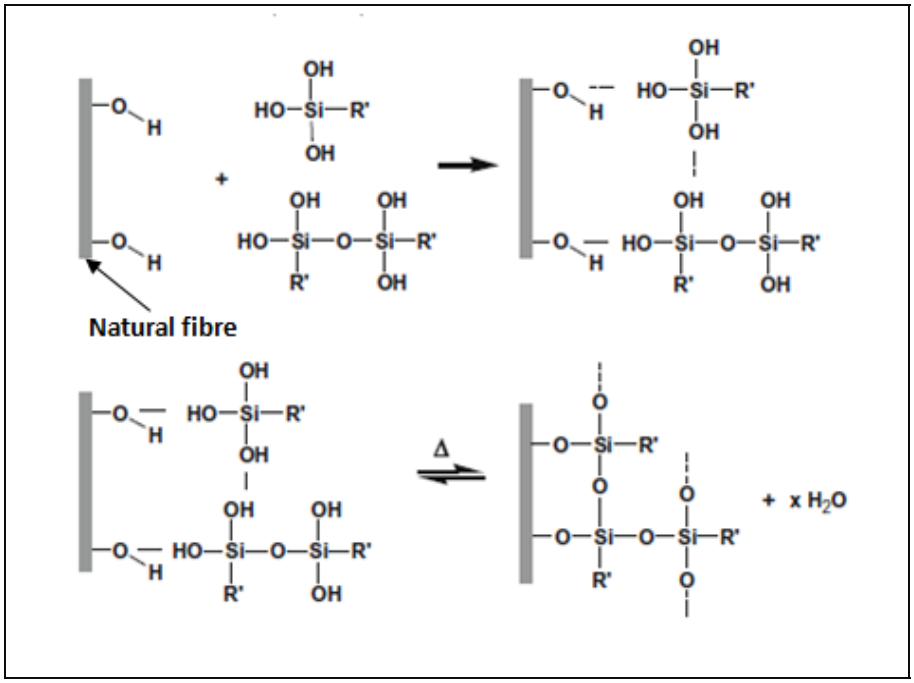

Figure 2.4 Interaction of silane with natural fibres by chemical grafting

Huda *et al.* [40] investigated the mechanical and thermal properties of kenaf fibre reinforced poly(lactic acid) (PLA) laminated composites as a function of modification of kenaf fibre by using alkalization and silane treatments. The composites were prepared by compression molding using a film-stacking method. The results obtained showed that the silane coupling agent improved the compatibility between the kenaf fibre and PLA. The mechanical and thermo-mechanical properties of the PLA/kenaf composites were significantly better than

those of the PLA. This was believed to be caused by improved interfacial interaction, resulting in a high flexural stiffness. The silane pre-treatment enhanced the composites' mechanical properties in comparison with the composites containing untreated kenaf fibre.

Devi *et al*. [41] investigated the tensile, flexural, and impact behaviour of pineapple leaf fibre (PALF) reinforced polyester composites as a function of fibre loading, fibre length, and fibre surface modification. A comparison of the effect of two silane coupling agents on the mechanical properties was carried out. A 40% increase in the tensile strength was observed when the fibres were treated with silane A172 (vinyltri(2-ethoxymethoxy)silane). The flexural strength of these composites also increased by about 7%. In the silane A172-treated composites, the alkoxy group of silane hydrolyzes to form silanols (-OH). This -OH group interacts with the -OH groups of lignocellulosic PALF, forming hydrogen bonds, and the vinyl group reacts with the polyester. This would cause the resin to be less interconnected, resulting in a higher elongation of the silane-treated composites. Addition of the coupling agent silane A1100 (γ-aminopropyltrimethoxysilane) improved the Young's modulus of the composites only marginally. However, other properties were unaffected.

Abdelmouleh *et al.* [42] studied the surface modification of cellulosic fibres carried out using organofunctional silane coupling agents in an ethanol/water medium. Heat treatment (curing) was applied after reaching the equilibrium adsorption of the pre-hydrolysed silanes onto the cellulosic substrate. The modified fibres were then characterised by diffuse reflectance infrared spectroscopy and contact angle measurements. The presence of Si–O–cellulose and Si–O–Si bonds on the cellulose surface confirmed that the silane coupling agent was efficiently held on the fibre surfaces through both condensation with cellulose hydroxyl groups and self-condensation between silanol groups. The change of the surface properties after the modification was determined by contact angle measurements and inverse gas chromatographic analysis. It was shown that the silane functional groups, attached to the fibre surface, could participate in the chain growth of appropriate monomers to give a covalent continuity between the fibres and the resulting polymer matrix.

2.3 Biopolymers

2.3.1 Biodegradable polymers

In recent years, there has been a marked increase in interest in biodegradable materials for use in agricultural, medicine, packaging, and other areas. In particular, biodegradable polymer materials (known as biopolymers) are of interest to many researchers. Since polymers form the backbone of plastic materials, they are continually being employed in an expanding range of areas. As a result, many researchers are investing time into modifying traditional materials, to make them user-friendly and to design novel polymer composites out of naturally occurring materials [17,31,43]. Biodegradable polymers are plastics obtained from renewable resources synthesized from petroleum-based chemicals, and which can be degraded by microorganisms. They are capable of undergoing decomposition when exposed to environmental conditions [2]. Polymer materials are classified into three primary classes, which define their degradation behaviour. The first class is the conventional plastics, that are resistant to degradation when disposed into the natural environment. The resistance to degradation is due to their impenetrable petroleum based matrix, which is reinforced with carbon or glass fibres and it is unable to be consumed by microorganisms. The second class of polymer materials are partially degradable. The production of these materials typically includes naturally produced fibres with a traditional matrix. When exposed to environmental conditions, microorganisms are able to consume the natural macromolecules within the plastic matrix, leaving the matrix weakened with rough and open edges, resulting in further degradation. The final class of polymer materials is completely biodegradable; the polymer matrix is derived from natural resources such as starch or microbial grown polymers, and their reinforcement is produced from common crops such as flax, kenaf or hemp. According to the American society for Testing of Materials (ASTM), biodegradable polymers are defined as those that undergo a significant change in chemical structure under specific environmental conditions [17], such as photodegradation, hydrolysis, oxidation and microbial induced chain scission, leading to mineralization which alters the polymer during the degradation process. They are capable of undergoing decomposition primarily through enzymatic action of microorganisms (fungi, algae, bacteria, etc.) into CO_2, methane, biomass or inorganic compounds in a specified period of time [2,17,31].

2.3.2 Degradation of biopolymers by microorganisms

Biodiversity and occurrence of polymer-degrading microorganisms vary depending on the environment, such as soil, sea, compost, and activated sludge. It is necessary to investigate the distribution and population of polymer-degrading microorganisms in various ecosystems. Generally, the adherence of microorganisms on the surface of plastics, followed by the colonization of the exposed surface, is the major mechanism involved in the microbial degradation of plastics. The enzymatic degradation of plastics by hydrolysis is a two-step process: (i) the enzyme binds to the polymer substrate then subsequently catalyzes a hydrolytic cleavage. Polymers are degraded into low molecular weight oligomers, dimers and monomers, and finally mineralized to CO_2 and H_2O; (ii) the clear zone method with agar plates is a widely used technique for screening polymer degraders and for assessment of the degradation potential of different microorganisms on a polymer. Agar plates containing emulsified polymers are inoculated with microorganisms and the presence of polymer degrading microorganisms can be confirmed by the formation of clear halo zones around the colonies. This happens when the polymer-degrading microorganisms excrete extracellular enzymes which diffuse through the agar and degrade the polymer into water soluble materials. Through several studies, researchers investigated the population of aliphatic polymer-degrading microorganisms in different ecosystems, and the degradation order was found to be as follows: PHB = PCL > PBS > PLA were, poly(3-hydroxybutyrate)-(PHB), poly(ε-caprolactone)-(PCL), poly(butylene succinate)-(PBS) and poly(lactic acid)-(PLA) [11,44-47].

In the last years there was a remarkable interest in polymers that undergo controlled biological degradation by microorganisms. The polymers may contribute to the solution of problems arising from plastic waste disposal. Within this group of innovative polymers, polyesters play a predominant role, due to their potentially hydrolysable ester bonds. While aromatic polyesters such as poly(ethylene terephthalate) exhibit excellent material properties, they proved to be almost resistant to microbial attack. Aliphatic polyesters, however, are biodegradable but lack the important properties for many applications. Therefore, aliphatic-aromatic copolyesters were created to combine good material properties with biodegradability. The biodegradability of polymers is not only dependent on the presence of functional groups and a hydrophilicity-hydrophobicity balance, but also on the ordered structure such as orientation, crystallinity and other morphological properties. It has been

shown that copolyesters containing adipic acid and terephthalic acid as aromatic acid components are generally attacked by microorganisms. [6,10,48-50].

Teramoto *et al.* [8] investigated the biodegradability of the composites of aliphatic polyesters (PCL, poly(3-hydroxybutyrate-co-3-hydroxyvalerate (PHBV), PBS and PLA) with untreated abaca and acetic anhydride-treated abaca (AA-abaca) fibres by a soil burial test. They observed that for neat polyesters the order of highest weight loss after burial was PCL > PHBV > PBS > PLA. The weight loss of PCL after 180 days was 45%, while no weight loss was observed for PLA. In the case of PCL composites, the presence of untreated abaca or AA-abaca did not have a pronounced affect on the weight loss, because PCL itself has a relatively high biodegradability. However, the addition of abaca fibres accelerated the weight loss process in the case of PHBV and PBS composites. Especially, when untreated abaca was used, the PHBV and PBS composite specimens crumbled within 3 months. No weight loss was observed for the neat PLA and the PLA/AA-abaca composite, while the PLA/untreated abaca composite showed 10% weight loss after 60 days. The weight loss of the abaca composite was caused by the preferential degradation of abaca fibre through the cracks of the composite surface. Such cracks were not observed when surface-modified AA-abaca was used.

Kumar *et al.* [15] studied the biodegradation of flax fibre reinforced PLA. Woven and nonwoven fibre biocomposites were prepared with amphiphilic additives as accelerator for biodegradation. The composites were buried in farmland soil for biodegradability studies. The loss in weight of the biodegraded composite samples was determined at different time intervals. The surface morphology of the biodegraded composites was studied with scanning electron microscopy (SEM). The results indicated that in the presence of mandelic acid, the composites showed accelerated biodegradation with 20–25% weight loss after 50–60 days. On the other hand, in presence of dicumyl peroxide the biodegradation of the composites was relatively slow as confirmed by only 5–10% weight loss after 80–90 days. This was further confirmed by the surface morphology of the biodegraded composites.

Kiatkamjornwong *et al.* [19] studied starch-g-polystyrene copolymers prepared by simultaneous irradiation of starch and styrene by γ-rays from a ^{60}Co-source. The grafted copolymers were used for studies on the degradation of the plastic. A mixture of starch, styrene and methanol was irradiated by gamma rays to various total doses ranging from 2 to

16 kGy at a fixed dose rate of 2.5×10^{-3} kGy s^{-1}. The copolymers were characterized in terms of the homopolymer content, grafting efficiency, grafting ratio, conversion, and percentage add-on. The highest percentage of grafting efficiency (62.2%) was obtained at a total dose of 10 kGy. The effect of nitric acid inclusion for enhancing the grafting of styrene onto cassava starch was also studied. Polystyrene (PS) cannot disintegrate naturally by itself. The degradation of polystyrene containing cassava starch and graft copolymers was investigated by outdoor exposure, soil burial testing, and UV irradiation. The degradation processes were followed by monitoring tensile properties, an index of the extent of degradation, carbonyl index, molecular weight changes, and thermal properties of the plastic. It was found that the physical properties of graft copolymer-filled PS sheets rapidly deteriorated upon outdoor exposure, or UV irradiation as evidenced by calculated activation energies of plastic decomposition. The PS containing the graft copolymer needed less activation energy to start the decomposition process than the control PS. There were no samples that significantly degraded upon indoor exposure. All plastics took a longer time to degrade by the soil burial test. *Bacillus coagulans* 352 was used to test the biodegradability resistance of the plastic sheets to bacteria. The composite PS sheets revealed destroyed areas of starch, indicating that bacteria help promote the biodegradation of polystyrene plastics before other disintegrations take place.

2.3.3 Factors affecting the biodegradability of biopolymers

Biopolymers were originally designed for the packaging and farming sector, because they were not suitable to be used as matrices in biocomposites. In particular, they show either too high values of elongation at failure, or their rheological behaviour is a strong restriction for application in biocomposites. The performance limitation and high cost of biopolymers are major barriers for their widespread acceptance as substitutes for traditional non-biodegradable polymers. The high cost of biopolymers compared to traditional plastics is mainly attributed to the low volume of production rather than the raw material costs for biopolymer synthesis. However, biopolymers are now of interest due to the current environmental threat and social concerns. New applications for these bio-based materials will result in increased production of biocomposites. The development of biodegradable polymers is challenging in view of the fact that such materials should be stable during storage and usage, and should degrade once disposed after their intended life time. Bioplastic modifications are applied to make the polymer a suitable matrix for composite applications. Reinforcing biopolymers with biofibres

can produce novel biocomposites to replace or substitute glass fibre-reinforced composites in various applications [43,44].

The properties of bioplastics are associated with their biodegradability. Both the chemical and physical properties of bioplastics influence the mechanism of biodegradation. The surface conditions (surface area, as well as hydrophilic and hydrophobic properties), the first order structures (chemical structure, molecular weight, molecular weight distribution), and the higher order structures (glass transition temperature, melting temperature, modulus of elasticity, crystallinity, crystal structure) of polymers play important roles in the biodegradation processes. In general, polyesters without side chains have better properties than those with side chains. The molecular weight is also important for the biodegradability because it determines many physical properties of the polymer. Increasing the molecular weight of the polymer decreases its degradability. Investigations on polycaprolactone (PCL) with higher molecular weight (M_n > 4,000) showed that it degraded slower than the lower molecular weight polymer [20]. The morphology of polymers also affects their rates of biodegradation. The degree of crystallinity is a crucial factor affecting biodegradability, since enzymes mainly attack the amorphous domains of a polymer. The molecules in the amorphous region are loosely packed, and therefore make it more susceptible to degradation. The crystalline part of the polymers is more resistant than the amorphous part. Iwata and Tsuji [20,21,44] reported that the rate of degradation of PLA decreases with an increase in the crystallinity of the polymer.

The melting temperature of polyesters has a strong effect on the enzymatic degradation of the polymers. The aliphatic polyesters (ester bond (-CO-O-)) and polycarbonates (carbonate bond (-O-CO-O-)) are two typical plastic polymers that have a good potential for use as biodegradable plastics, owing to their susceptibilities to lipolytic enzymes and microbial degradation. Compared with aliphatic polyesters and polycarbonates, aliphatic polyurethane and polyamides (nylon) have higher melting temperatures, resulting in lower biodegradability properties [44].

2.4 Copolyester/natural fibre biocomposites

Different techniques have been used to prepare copolyester/natural fibre biocomposites. These techniques include solution mixing, roll milling, melt mixing, as well as injection and

compression moulding [35,36,40,51]. The methods differ in terms of their operating principles and processing parameters, which may lead to fairly different properties of the prepared composites. Analysis/characterization can be carried out in terms of thermal properties, mechanical and thermomechanical properties, and morphology. Copolyester/natural fibre biocomposites were generally pre-treated on the surface of the fibre or incorporated with surface modifiers to improve the interfacial adhesion between the hydrophilic natural fibres and the hydrophobic copolyester. This can be achieved by using treatments such as silane coupling agents, mercerization, and compatibilizers [22-42,52-55].

2.4.1 Morphology

Many studies that have been carried out focused on the morphology of non-treated and treated composites or biocomposites. Huda *et al.* [40] focused on untreated and treated PLA/kenaf fibre biocomposites. The kenaf fibre was modified by using alkalization and silane treatments. The biocomposites were prepared by compression moulding using a film-stacking method. Scanning electron microscopy (SEM) was used to investigate fractured surfaces of the samples. Composites with untreated fibre had fibre pull-outs, indicating a low fibre/matrix adhesion. Good surface adhesion was only observed for treated fibre composites, showing that kenaf fibre was well trapped by the PLA matrix. This observation indicates that the changes of the surface topography affect the interfacial adhesion. Silane treatment increased the adhesion of the PLA matrix to the kenaf fibres. The coupling agent caused significantly better wetting of the kenaf fibre by the matrix. Similar behaviour was observed for neat Solanyl (copolyester) and jute fibre biocomposites investigated by Lee *et al.* [56]. The biocomposites were compounded in a twin screw extruder after the jute fibre was treated with 5% NaOH for 8 hours. The SEM micrographs showed poor interfacial adhesion and inadequate wetting of the untreated fibres with the Solanyl matrix.

Keller [57] investigated biodegradable hemp fibre composites. The hemp fibre bundles used for the composites were degummed by means of biological processes (BIA) and steam explosion (DDA). The degummed fibres, separated into single cells, were integrated into the brittle poly(3-hydroxybutyrate-co-hydroxyvalerate) (PHBV) matrix and into the ductile co-polyester amide (PEA) matrix by means of a co-rotating twin screw extruder and compression moulded to test samples. The fractured surfaces were analysed by scanning electron microscopy. The SEM photos of the PEA–DDA and PHBV–BIA composites showed fibres

with no adhering matrix fragments on the surface. The fracture ran along the interface between fibre and matrix, indicating low fibre–matrix adhesion. The debonding energy was therefore low and fibre pull-out prevailed over fibre fracture.

Mehta *et al*. [58] investigated the effect of fibre surface treatment on the properties of biocomposites. Nonwoven industrial hemp fibre mats and unsaturated polyester resin were prepared by compression moulding. The fibres were treated using alkali, silane, an unsaturated polyester resin matrix, and acrylonitrile treatments. The morphology of the untreated and surface-treated hemp fibres were investigated by SEM analysis. The distribution of the fibres in the hemp mat was random, and uneven. Fibrillation was observed in fibres after surface treatment. This could provide more anchorage for the matrix, and hence improve the strength of the composite. In general, the surface of chemically treated fibres looked different from that of the untreated hemp fibre. In the biocomposites, fibre pull-out was clearly observed. The biocomposite with untreated hemp fibres showed poor interfacial bonding between the fibre and the matrix, which resulted in a relatively clean surface of the pulled out fibres due to a greater extent of delamination. In the case of the untreated fibre-based biocomposites, shear failure resulted in a high degree of pull-out. The adhesion between the fibre and the matrix was enhanced in biocomposites with surface-treated fibres. The fibres were covered with the matrix, and the fibre pull-out was relatively smaller.

2.4.2 Thermal properties

The investigations on the thermal properties of the copolyester/natural fibre composites were generally conducted by comparing the degradation behaviour of natural fibre, virgin copolyester, and untreated copolyester/natural fibre composites compared to the treated composites. In most cases the treated composites showed higher thermal stability than both the untreated composites and the pure components.

Rudnik *et al.* [59] studied the thermal properties of new biocomposites prepared from a modified starch matrix reinforced with natural vegetable fibres. Differential scanning calorimetry (DSC) and thermogravimetric analysis (TGA) were used to study the thermal behaviour of the biocomposites. The biocomposites were compounded using a twin-screw extruder. Two kinds of natural fibres were used, flax and cellulose in amount of 0-40 mass %. The DSC curves of the biocomposites revealed a glass transition temperature of 69 °C for the

amorphous plasticized starch. The authors reported an increase in the glass transition for starch rich phase from 69 to 118 °C after incorporation of natural fibres. Avérous *et al.* [60] reported an increase in the glass transition for the plasticized starch matrix reinforced with leafwood cellulose fibres, determined by dynamic mechanical analysis, from 31 to 59 °C for the sample containing 10 wt% fibres. The T_g showed a further, but smaller, increase when the fibre content was increased from 10 to 18 wt%. Although the results from these two papers seem to support each other, I am not completely convinced about the correctness of the T_g values reported by Rudnik *et al.* [59]. These values were obtained from DSC curves that show only very weak changes in the baseline that were not nearly as well resolved as the DMA relaxations observed by Avérous *et al.* [60]. The thermal stability of the biocomposites was determined from the temperature at which 5% mass loss occurred. For the plasticized starch the degradation started at 168 °C, whereas the biocomposites started to decompose at 188 and 176 °C respectively for flax and cellulose reinforced biocomposites. The increase in thermal stability with introduction of natural fibre was observed for both flax and cellulose reinforced biocomposites.

Krishnaprasad *et al.* [61] investigated the thermal properties of bamboo reinforced polyhydroxybutyrate (PHB) biocomposites. Composites based on PHB and bamboo microfibrils were prepared with various microfibril loadings by using a micro compounder. The TGA results showed that the thermal stability of the composites was higher than that of pure PHB, and the thermal stability of PHB was improved by incorporation of bamboo microfibrils.

2.4.3 Mechanical and thermomechanical properties

The incorporation of natural fibres into a polymer is known to cause substantial changes in the mechanical properties of the composites. The quality of the fibre-matrix interaction is important for the application of natural fibres as reinforcement for polymers. Better interaction can only be achieved through introduction of compatibilizers to or chemical modification of the natural fibre and the polymer [2,18-20,43-55,62-65]. A number of studies reported on the effect of poor or good interfacial adhesion on the mechanical and viscoelastic properties of the copolyester/natural fibre biocomposite materials.

Ochi [67] investigated the mechanical properties of kenaf fibre and kenaf/PLA composites. The biodegradable composite specimens were prepared by using a hot melt press. The results obtained showed a linear increase in the tensile strength for fibre contents up to 50%. At 70% fibre content the tensile strength obtained was lower. This was because of voids and fibre-fibre contact caused by an insufficient amount of resin. The tensile strengths of these composites were much higher compared to the values reported by Nishino *et al*. [68] for kenaf/PLA composites. The difference in the tensile strength was attributed to better moulding conditions, which prevented strength reduction due to thermal degradation. Furthermore, fabrication with an emulsion-type-biodegradable resin contributed to the reduction of voids and fibre contacts in the composites.

Krishnaprasad *et al.* [61] investigated the mechanical properties of PHB and its composites with bamboo fibre with varying fibril loading. The tensile strength of 5 parts by weight (pbw) microfibril containing PHB was lower than that of pure PHB. This was due to the lower loading of microfibrils being insufficient to reinforce the PHB matrix, and which acted as flaws or stress concentration points. With a further increase in microfibril loading, the tensile strength increased and reached a maximum at a fibre loading of 20 pbw. Further increases in fibre loading reduced the tensile strength.

Huda *et al.* [40] investigated the thermomechanical properties of kenaf fibre reinforced poly(lactic acid) (PLA) laminated composites as a function of modification of kenaf fibre by using alkali and silane treatments. The storage (elastic) modulus, loss modulus, and loss factor were determined by dynamic mechanical analysis (DMA). The storage modulus of the composites was higher than that of the PLA matrix, due to the reinforcement effect of the kenaf fibres. The alkali treated fibre (FIBNA) composite had higher storage moduli than the untreated fibre (FIB) composite. This suggested that the adhesion between the PLA matrix and the kenaf fibres was better with NaOH treated kenaf rather than with the untreated kenaf. The removal of lignin was therefore a key step in producing high modulus composites. The effect of 3-aminopropyltriethoxysilane (APS) pre-treatment on the storage modulus of the composites was investigated by comparing PLA/FIB with PLA/FIBSI, and PLA/FIBNA with PLA/FIBSI. The storage modulus increased with 41%, 67% and 87% respectively for the FIB, FIBNA and silane-treated (FIBSI) composites, when compared to neat PLA at 25°C. The storage modulus decreased with increasing temperatures for all the samples, and there was a significant decrease in the region between 50 and 70°C. The surface-treated fibre reinforced

composites showed a longer plateau on the storage modulus curve than neat PLA, where the softening temperature increased from about 48 °C for neat PLA to 57 °C for the composite with kenaf fibres. The viscoelastic properties of neat PLA, untreated and treated fibre reinforced composites were also studied. The T_g of both FIBSI and FIBSINA reinforced composites shifted to higher temperatures because of the silane-treated fibre present in the PLA matrix. It was found that the T_g for neat PLA was around 63 °C and increased to 68 °C for FIBSI and 67 °C for alkali- followed by silane-treated fibre (FIBNASI). The increase in T_g was explained based on the retardation in the relaxation of the amorphous regions, due to the physical interaction between the reinforcing phase and the crystalline regions of the PLA matrix. The fibres' contribution to the damping was extremely low compared to that of the PLA matrix observed from tan δ. This suggests that the combined attenuation of kenaf fibre reinforced composites would be mainly caused by the molecular motion of PLA and the interaction at the fibre/matrix interface. Moreover, the removal of the lignin in the FIBNA and FIBNASI fibres led to a change in the extent of hydrogen-bonding, affecting the tan δ of the composites.

Oksman *et al*. [52] investigated natural fibre reinforced poly(lactic acid) (PLA) composites. The composites were manufactured with a twin-screw extruder, and had flax fibre contents of 30 and 40 mass %. The extruded composites were compression moulded to test samples. The storage modulus and tan δ of the pure PLA and the PLA/flax composites were determined by DMA analysis. It was observed that the thermal properties of PLA improved with the incorporation of flax fibres. The softening temperature increased from about 50 °C for pure PLA to 60 °C for the composites, and it further increased when the composite was crystallized. The composites softened after 60 °C, but the modulus started to increase again around 80 °C, which was a typical effect of cold crystallisation. The crystallized sample (PLA/flax II) showed very good thermal properties. The tan δ curves for the PLA, PLA/flax and PLA/flax II (cold crystallised) composites showed that the tan delta peak did not change due to the addition of flax, but that it was affected by the crystallisation.

2.5 References

1. J.C. Huang, A.S. Shetty, M.S. Wang. Biodegradable plastics. Advances in Polymer Technology 1990; 10:23-30.
2. A.K. Mohanty, M. Misra, L.T. Drzal. Sustainable bio-composites from renewable resources: Opportunity and challenges in the green material world. Journal of Polymers and the Environment 2002; 10:19-26.
3. S. Alix, S. Maris, C. Morvan, L. Lebrun. Biocomposite materials from flax plants: Preparation and properties. Composites Part A 2008; 39:1793-1801.
   DOI: 10.1016/j.compositesa.2008.08.008
4. P. Mukhopadhyay. Emerging trends in plastic technology. Plastics Engineering 2002; 58:28-35.
5. M. Avella, A. Buzarovska, M. E. Errico, G. Gentile, A. Grozdanov. Eco-challenges of bio-based polymer composites. Materials 2009; 2:911-925.
   DOI: 10.3390/ma2030911
6. A. Steinbuchel. Biopolymers, general aspects and special applications. Biopolymers. 2003; 10:516-518.
7. D.R. Lu, C.M. Xiao, S.J. Xu. Starch-based completely biodegradable polymer materials. eXPRESS Polymer Letters 2009; 3:366-375.
   DOI: 10.3144/expresspolymlett.2009.46
8. N. Teramoto, K. Urata, K. Ozawa, M. Shibata. Biodegradation of aliphatic polyester composites reinforced by abaca fibre. Polymer Degradation and Stability 2004; 86:401-409.
   DOI: 10.1016/j.polymdegradstab.2004.04.026
9. F. Chivrac, Z. Kadlecová. E. Pollet, L. Avérous. Aromatic copolyester-based nano-biocomposites: Elaboration, structural characterization and properties. Journal of Polymers and the Environment 2006; 14:393-401.
   DOI: 10.1007/s10924-006-0033-4
10. Y. Chen, L. Tan, L. Chen, Y. Yang, X. Wang. Study on biodegradable aromatic-aliphatic copolyesters. Brazilian Journal of Chemical Engineering 2008; 25:321-335.
11. G. Seretoudi, D. Bikiaris, C. Panayiotou. Synthesis, characterization and biodegradability of poly(ethylene succinate)/poly(1-caprolactone) block copolymers. Polymer 2002; 43:5405-5415.

12. A. Bhatia, R.K. Gupta, S.N. Bhattacharya, H.J. Choi. Compatibility of biodegradable poly(lactic acid) (PLA) and poly(butylene succinate) (PBS) blends for packaging application. Korea-Australia Rheology Journal 2007; 19:125-131.
13. H.-Y. Cheung, K.-T. Lau, X.-M. Tao, D. Hui. A potential material for tissue engineering: Silkworm silk/PLA. Composites Part B 2008; 39:1026–1033.
14. T. Ishigaki, W. Sugano, M. Ike, Y. Kawagoshi, I. Fukunaga, M. Fujita. Abundance of polymers degrading microorganisms in a sea-based solid waste disposal site. Journal of Basic Microbiology 2000; 40:177-186.
15. R. Kumar, M.K. Yakubu, R.D. Anandjiwala. Biodegradation of flax fibre reinforced poly(lactic acid). eXPRESS Polymer Letters 2010; 4:423-230.
DOI: 10.3144/expresspolymlett.2010.53
16. D. Plackett, T.L. Andersen, W.B. Pedersen, L. Nielsen. Biodegradable composites based on L-polylactide and jute fibres. Composites Science and Technology 2003; 63:1287-1296.
DOI: 10.1016/S0266-3538(03)00100-3
17. M. Kolybaba, L.G. Tabil, W.J. Crerar, B. Wang. Biodegradable polymers: Past, present and future. The Society for Engineering in Agricultural, Food and Biological Systems, ASAE meeting presentation. Fargo, North Dakota, USA. 3-4 October 2003.
18. I. Vroman, L. Tighzert. Biodegradable polymers. Materials 2009; 2:307-344. DOI:10.3390/ma2020307
19. S. Kiatkamjornwong, M. Sonsuk, S. Wittayapichet, P. Prasassarakich, P.-C. Vejjanukroh. Degradation of styrene-g-cassava starch filled polystyrene plastics. Polymer Degradation and Stability 1999; 66:323-335.
DOI: 10.1016/S0141-3910(99)00082-8
20. T. Iwata, Y. Doi. Morphology and enzymatic degradation of poly(L-lactic acid) single crystals. Macromolecules 1998; 31:2461-2467.
DOI: 10.1021/ma980008h
21. H. Tsuji, S. Miyauchi. Poly(L-lactide) 6. Effects of crystallinity on enzymatic hydrolysis of poly(l-lactide) without free amorphous region. Polymer Degradation and Stability 2001; 71:415-424.
22. G.R. Laghtsey. Organic fillers for thermoplastics. Polymer Science and Technology 1983; 17:193-211.
23. I. Krupa, A.S. Luyt. Thermal properties of polypropylene/wax blends. Thermochimica Acta 2001; 372:137-141.

DOI: 10.1016/S0040-6031(01)0045-6

24. E.T.N. Bisanda, M.P. Ansell. The effect of silane treatment on the mechanical and physical properties of sisal-epoxy composites. Composites Science and Technology 1991; 41:165-178.
DOI: 10.1016/0266-3538(91)90026-L
25. C. Pavithran, P.S. Mukherjee, M. Bramakumar, A.D. Damodaran. Impact properties of natural fibre composites. Journal of Materials Science Letters 1987; 7:882-889.
26. I.K. Varma, S.R. Anantha Krishnan, S. Krishnamoorthy. Composites of glass/modified jute fabric and unsaturated polyester resin. Composites 1989; 20:383-388.
DOI: 10.1016/0010-4361(89)90664-2
27. A. Valadez-Gonzalez, J.M. Cervantes-Uc, R. Olayo, P.J. Herrera-Franco. Effects of fiber surface treatment on the fiber-matrix bond strength of natural fiber reinforced composites. Composites Part B 199; 30:309-320.
28. S.C. Turmanova, S.D. Genieva, A.S. Dimitrova, L.T. Vlaev. Non-isothermal degradation kinetics of filled with rise husk ash polypropene composites. eXPRESS Polymer Letters 2008; 2:133-146.
DOI: 10.3144/expresspolymlett.2008.18
29. A.K. Mohanty, M. Misra, L.T. Drza. Surface modification of natural fibres and performance of the resulting biocomposites. Composite Interfaces 2001; 8:313-343.
DOI: 10.1163/156855401753255422
30. A.C.N. Singleton, C.A. Baillie, P.W.R. Beaumont, T. Peijs. On the mechanical properties, deformation and fracture of a natural fibre/recycled polymer composite. Composites: Part B 2003; 34:519-526.
DOI: 10.1016/S1359-8368(03)00042-8
31. A.K. Mohanty, M. Misra, G. Hinrichsen. Biofibres, biodegradable polymers and biocomposites: An overview. Macromolecular Materials and Engineering 2000; 276/277:1-24.
32. T.W. Frederic, W. Norman. Natural fibres plastics and composites. Kluwer Academic Publishers: New York (2004).
ISBN: 1 4020 7643 6
33. X. Li, L.G. Tabil, S. Panigrahi. Chemical treatments of natural fibre for use in natural fibre-reinforced composites. Journal of Polymers and the Environment 2007; 15:25-33.
DOI: 10.1007/s10924-006-0042-3

34. W. Liu, A.K. Mohanty, P.A. L.T. Drzal, M. Misra. Influence of fiber surface treatment on properties of Indian grass fiber reinforced soy protein based biocomposites. Polymer 200; 45:7589-7596.
DOI: 10.1016/j.polymer.2004.09.009

35. A.M. Mohd Edeerozey, H. Md Akil, A.B. Azhar, M.I. Zainal Ariffin. Chemical modification of kenaf fibres. Materials Letters 2007; 61:2023–2025.
DOI: 10.1016/j.matlet.2006.08.006

36. W.L. Lai, M. Mariatti, S. Mohamad Jani. The properties of woven kenaf and betel palm (*Areca catechu*) reinforced unsaturated polyester composites. Polymer-Plastics Technology and Engineering 2008; 47:1193-1199.
DOI: 10.1080/03602550802392035

37. N.A. Ibrahim, K.A. Hadithon, K. Abdan. Effect of fibre treatment on mechanical properties of kenaf-Ecoflex composites. Journal of Reinforced Plastics and Composites 2010; 29:2921-2198.
DOI: 10.1177/0731684409347592

38. H.A. Sharifah, P.A. Martin. The effect of alkalization and fibre alignment on the mechanical and thermal properties of kenaf and hemp bast fibre composites: Part 1 – polyester resin matrix. Composites Science and Technology 2004; 64:1219–1230.
DOI: 10.1016/j.compscitech.2003.10.001

39. Y. Xie, C.A.S. Hill, Z. Xiao, H. Militz, C. Mai. Silane coupling agents used for natural fibre/polymer composites. Composites Part A 2010; 41:806–819.

40. M.S. Huda, L.T. Drzal, A.K. Mohanty, M. Misra. Effects of fibre surface-treatments on the properties of laminated biocomposites from poly(lactic acid) (PLA) and kenaf fibres. Composites Science and Technology 2008; 68:424-432.
DOI: 10.1016/j.compscitech.2007.06.022

41. L.U. Devi, S.S. Bhagawan, S. Thomas. Mechanical properties of pineapple leaf fibre-reinforced polyester composites. Journal of Applied Polymer Science 1997; 64:1739-1748.

42. M. Abdelmouleh, S. Boufi, M.N. Belgacem, A.P. Duarte, A.B. Salah, A. Gandini. Modification of cellulosic fibers with functionalized silanes: Effect of the fiber treatment on the mechanical performance of cellulose-thermoset composites. Journal of Applied Polymer Science 2005; 98:974-984.
DOI: 10.1002/app.22133

43. U. Riedel. Natural fibre-reinforced biopolymers as construction materials – new discoveries. 2nd International Wood and Natural Fibre Composites Symposium. Kassel, Germany 28-29 June 1999.
44. Y. Tokiwa, B.P. Calabia, C.U. Ugwu, S. Aiba. Biodegradability of Plastics. Molecular Sciences 2009; 10:3722-3724.
DOI: 10.3390/ijms10093722
45. A. Bhatia, R.K. Gupta, S.N. Bhattacharya, H.J. Choi. Compatibility of biodegradable poly(lactic acid) (PLA) and poly(butylene succinate) (PBS) blends for packaging application. Korea-Australia Rheology Journal 2007; 19:125-131.
46. H.-Y. Cheung, K.-T. Lau, X.-M. Tao, D. Hui. A potential material for tissue engineering: Silkworm silk/PLA. Composites Part B 2008; 39:1026–1033.
47. T. Ishigaki, W. Sugano, M. Ike, Y. Kawagoshi, I. Fukunaga, M. Fujita. Abundance of polymers degrading microorganisms in a sea-based solid waste disposal site. Journal of Basic Microbiology 2000; 40:177-186.
48. T. Nakajima-Kambe, F. Ichihashi, R. Matsuzoe, S. Kato, N. Shintani. Degradation of aliphatic-aromatic copolyester by bacteria that can degrade aliphatic polyesters. Polymer Degradation and Stability 2009; 94:1901-1905.
DOI: 10.1016/j.polymdegradstab.2009.08.006
49. I. Kleeberg, C. Hetz, R.M. Kroppenstedt, R.-J. Muller, W.-D. Deckwer. Biodegration of aliphatic-aromatic copolyesters by *Thermomonospora fusca* and other Thermophilic Compost Isolates. Applied and Environmental Microbiology 1998; 64:1731-1735.
50. S. Mohanty, S. K. Nayak. Aromatic-aliphatic poly(butylene adipate-co-terephthalate) bionanocomposites: Influence of organic modification on structure and properties. Polymer Composites 2010; 31:1194-1204.
DOI: 10.1002/pc.20906
51. G. Mehta, L.T. Drzal, A.K. Mohanty, M. Misra. Effect of fibre surface treatment on the properties of biocomposites from nonwoven industrial hemp fibre mats and unsaturated polyester resin. Journal of Applied Polymer Science 2006; 99:1055–1068.
DOI: 10.1002/app.22620
52. K. Oksman, M. Skrifvars, J.-F. Selin. Natural fibres as reinforcement in polylactic acid (PLA) composites. Composites Science and Technology 2003; 63:1317–1324.
DOI: 10.1016/S0266-3538(03)00103-9
53. S. Taj, M.A. Munawar, S. Khan. Natural fibre-reinforced polymer composites. Proceedings of the Pakistan Academy of Sciences 2007; 44:129-142.

54. R. Kozlowski, M. Wladyka-Przybylak. Flammability and fire resistance of composites reinforced by natural fibres. Polymers for Advanced Technologies 2008; 19:446-453.
DOI: 10.1002/pat.1135

65. P.A. Fowler, J.M. Hughes, R.M. Elias. Biocomposites: Technology, environmental credentials and market forces. Journal of the Science of Food and Agriculture 2006; 86:1781-1789.
DOI: 10.1002/jsfa.2558

56. M.W. Lee, S.Y. Ho, K.P. Lim, T.T. Ng, Y.K. Juay. Development of biocomposites with improved mechanical properties. SIMTech Technical Reports 2008; 9:115-118.

57. A. Keller. Compounding and mechanical properties of biodegradable hemp fibre composites. Composites Science and Technology 2003; 63:1307–1316.
DOI: 10.1016/S0266-3538(03)00102-7

58. G. Mehta, L.T. Drzal, A.K. Mohanty, M. Misra. Effect of fibre surface treatment on the properties of biocomposites from nonwoven industrial hemp fibre mats and unsaturated polyester resin. Journal of Applied Polymer Science 2006; 99:1055–1068.
DOI: 10.1002/app.22620

59. E. Rudnik. Thermal properties of biocomposites. Journal of Thermal Analysis and Calorimetry 2007; 88:495–498.
DOI: 10.1007/s10973-006-8127-8

60. L. Avérous, C. Fringant, L. Moro. Plasticized starch-cellulose interactions in polysaccharide composites. Polymer 2001; 42: 6565-6572.

61. R. Krishnaprasad, N. R. Veena, H.J. Maria, R. Rajan, M. Skrifvars, K. Joseph. Mechanical and thermal properties of bamboo microfibril reinforced polyhydroxybutyrate biocomposites. Journal of Polymers and the Environment 2009; 17:109-114.
DOI: 10.1007/s10924-009-0127-x

62. R.A. Cross, B. Kalra. Biodegradable polymers for the environment. Science Magazine 2002; 297:803-807.
DOI: 10.1126/science.297.5582.803

63. L. Liu, J. Yu, L. Cheng, X. Yang. Biodegradability of poly(butylene succinate) (PBS) composite reinforced with jute fibre. Polymer Degradation and Stability 2009; 94:90-94.
DOI: 10.1016/j.polymdegradstab.2008.10.013

64. V.A. Fomin. Biodegradable polymers, their present state and future prospects. Progress in Rubber and Plastics Technology 2001; 17:186-204.

65. A. Blanco. Just add water. Plastics Engineering 2002; 58:6.
66. S.T. Georgopoulos, P.A. Tarantili, E. Avgerinous, A.G. Andreopoloulos, E.G. Koukios. Thermoplastic polymers reinforced with fibrous agricultural residues. Polymer Degradation and Stability 2008; 90:303-312.
DOI: 10.1016/j.polymdegradstab.2005.02.020
67. S. Ochi. Mechanical properties of kenaf fibres and kenaf/PLA composites. Mechanics of Materials 2008; 40:446-452.
DOI: 10.1016/j.mechmat.2007.10.006
68. T. Nishino, K. Hirao, M. Kotera, K. Nakamae, H. Inagaki. Kenaf reinforced biodegradable composite. Composites Science and Technology 2003; 63:1281-1286.
DOI: 10.1016/S0266-3538(03)00099-X

CHAPTER THREE

EXPERIMENTAL

3.1 Materials

3.1.1 Kenaf fibre

Hibiscus cannabinus, commonly known as bast kenaf fibre, was obtained from Brits Textiles, South Africa. It has an average diameter of 0.078 mm, an average tensile strength of 488 MPa, and an average modulus of 24.6 MPa.

3.1.2 Aliphatic-aromatic copolyester

Ecoflex® F BX 7011, a biodegradable aliphatic-aromatic copolyester, with a melting temperature of 110-120 °C and a density of 1.25-1.27 g cm^{-3}, was supplied in pellet form by the BASF Chemical Company in South Africa.

3.1.3 Other chemicals

Sodium hydroxide was supplied in pellet form by Sigma-Aldrich, South Africa. It was a chemically pure (CP) grade with an assay of 99%, a density of 2.13 g cm^{-3} and a melting temperature of 318 °C.

A chemically pure (CP) grade silane coupling agent with an assay of 99.8%, a density of 1.064 g cm^{-3} and a boiling point of 211 °C was supplied by Sigma-Aldrich, South Africa

Disperal® 80 (Boehmite aluminium powder) from Sasol GmbH (Hamburg, Germany) was used as Disperal nanofiller. Its characteristics are listed in Table 3.1.

Table 3.1 Characteristics of Disperal

Properties	Unit	Disperal® 80
Al_2O_3- content	%	83.4
Surface area	$m^2 g^{-1}$	88.0
Loose bulk density	$g\ cm^{-3}$	0.38
Particle size: < 25 μm	%	48.6
Particle size: < 45 μm	%	80.7
Particle size: < 90 μm	%	100
Crystalline size (021)	Nm	74.4
Pore volume total	$mL\ g^{-1}$	0.870

3.2 Sample preparation methods

3.2.1 Alkali treatment

The chopped fibres of 5 mm length were placed in a stainless steel pot containing 4% sodium hydroxide (NaOH) solution and stirred well. This suspension was kept for 1 hour at room temperature with continuous stirring using a glass stirring rod. The fibres were then washed thoroughly with distilled water. The washing was repeated several times to remove the alkali. The fibres were finally washed with distilled water containing two drops of sulphuric acid. The treated kenaf fibres were allowed to dry in an air circulation air oven at 80 °C for 24 hours.

3.2.2 Silane coupling agent treatment

The alkali treated kenaf fibres were soaked for 5 minutes with continuous stirring in different concentrations of silane coupling agent (3%, 6% and 9%) prepared in 100 ml acetone at room temperature. After treatment the fibres were dried in an air circulation oven at 80 °C for 24 hours.

3.2.3 Modification of kenaf fibre with Disperal nano-powder

Silane modified fibres were divided into four portions of 100 g each. The fibres were immersed into a silane solution (100 ml silane and 3 ml acetone) mixed with different weight percentages of Disperal nano-powder (4, 6, 8 and 10 wt%) as an additive. The solutions were heated (60 °C) and stirred until all the powder was well mixed with the fibre. The modified fibres were dried in an air circulation oven at 80 °C for 24 hours. Table 3.2 summarizes the preparation and describes the notation of the composites.

Table 3.2 Abbreviations used for the different composites

Composite	Abbreviation
Matrix	
Aromatic-aliphatic copolyester	CP
Filler	
Untreated kenaf fibre	kenaf
4% NaOH treated kenaf fibre	NaOH-kenaf
3% silane treated kenaf fibre	NaOH-kenaf-silane3
6% silane treated kenaf fibre	NaOH-kenaf-silane6
9% silane treated kenaf fibre	NaOH-kenaf-silane9
3% silane + 4% Disperal treated kenaf fibre	NaOH-kenaf-silane3-Disperal4
3% silane + 6% Disperal treated kenaf fibre	NaOH-kenaf-silane3-Disperal6
3% silane + 8% Disperal treated kenaf fibre	NaOH-kenaf-silane3-Disperal8
3% silane + 10% Disperal treated kenaf fibre	NaOH-kenaf-silane3-Disperal10

3.2.4 Preparation of copolyester/kenaf fibre biocomposites

Copolyester/kenaf fibre biocomposites were prepared by a melt mixing process using a Haake Rheomix mixer at 150 °C at a speed of 60 rpm. for 8 min. The copolyester pellets were added first into the mixing chamber, followed by the modified fibres after a minute. The prepared samples were then melt pressed at 150 °C for 7 minutes under 50 bar into 2 mm thick sheets using a hot melt press.

3.3 Sample analysis

3.3.1 Tensile testing

A tensile test measures the force required to break a specimen and the extent to which the specimen stretches or elongates to that breaking point. It produces a stress-strain curve. The following calculations can be made from tensile test results: tensile strength (at yield and at break), tensile modulus, elongation and percent elongation at yield, and elongation and percent elongation at break. There are factors that should be taken into consideration whenever a test is carried out: (i) variability in the test results will be found due to variation in the sample material, sample preparation, test procedure and test machine accuracy; (ii) polymers are viscoelastic materials, therefore their properties are dependent on temperature, humidity, stretching speed or timescale of the test, and history of the sample; and (iii) tensile testing provides limited information, and therefore no accurate prediction of performance can be made without extensive product testing [1].

A Hounsfield H5KS universal testing machine was used for the tensile analysis of the samples. The dumbbell shaped samples (Figure 3.1) with a Gauge length of 24 mm, a thickness of 2 mm and width between 4.7 and 5.0 mm were tested at a speed of 5 mm min^{-1}. About five test specimens for each sample were analysed, and the averages and standard deviations of the different tensile properties are reported.

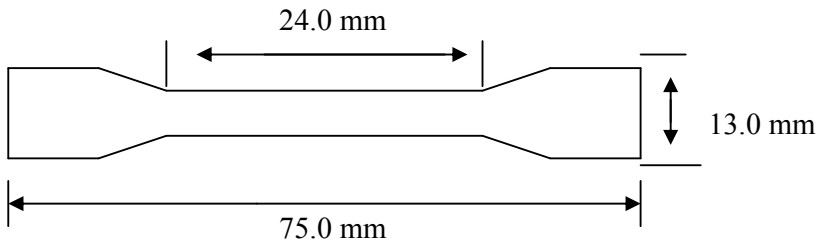

Figure 3.1 Dumbbell shaped tensile testing sample

3.3.2 Differential scanning calorimetry (DSC)

Differential scanning calorimetry is an analysis technique in which quantitative information on thermal transitions in materials may be obtained. DSC measures the heat required to maintain the same temperature in the sample versus an appropriate reference material in a furnace. Important physical changes in the sample that may be measured by DSC include melting temperature (T_m), crystallization temperature (T_c), glass transition temperature (T_g), and degradation or decomposition temperature (T_d). [1-3].

DSC analyses were performed in a Perkin-Elmer Diamond DSC with a hyper DSC thermal analyzer in flowing nitrogen atmosphere (20 ml min^{-1}). The samples having masses of 6-7 mg each were sealed in aluminium pans and heated from 30 to 200 °C at a rate of 10 °C min^{-1}. The melting peak temperatures and enthalpies were determined. The melting enthalpy calculated (ΔH_m^{cal}) was calculated from the experimental observed melting enthalpy (ΔH_m^{obs})$_{CP}$ of neat copolyester (CP) and weight the fraction of the polymer (W_{CP}) according to equation 3.1 [4].

$$\Delta H_m^{cal} = (\Delta H_m^{obs})_{CP} \times W_{CP} \qquad (3.1)$$

3.3.3 Thermogravimetric analysis (TGA)

Thermogravimetric analysis is a technique that uses heat to drive reactions and physical changes in materials providing quantitative measurements of any mass change in the polymer or material associated with a transition or thermal degradation. Mass change due to decomposition, oxidation or degradation of a polymer with time and temperature can be directly recorded from the TGA. TGA is mainly used to characterize the decomposition and thermal stability of materials under different conditions, and to examine the kinetics of the physico-chemical processes occurring in the sample. [1,2,5].

TGA analyses were performed in a Perkin-Elmer Pyris-1 TGA in flowing nitrogen atmosphere (20 ml min^{-1}). Samples with masses of 6-7 mg each were heated from 30 °C to 600 °C at a rate of 10 °C min^{-1}.

3.3.4 Dynamic mechanical analysis (DMA)

Dynamic mechanical analysis measures viscoelastic properties of materials. DMA determines changes in sample properties that result from changes in temperature, time, frequency, force and strain. The elastic modulus (storage modulus, E'), viscous modulus (loss modulus, E'') and damping coefficient (tan δ) as a function of time, temperature or frequency are used to determine how well a material will stand up to impact and stress relaxation. [1,2].

The samples were analysed using a Perkin-Elmer DMA-8000 analyser. The settings for the analyses were as follows:

Frequency	1 Hz
Amplitude	20 μm
Temperature range	-70 to 140 °C
Temperature program mode	Ramp
Measurement mode	Bending (dual cantilever)
Heating rate	2 °C min^{-1}
Preloading force	0.02 N
Sample length	15 mm
Sample width	9 mm
Sample thickness	2 mm

3.3.5 Biodegradability testing

The biodegradability test has been developed for the comparative investigation of different packaging materials and evaluation of their degradability in the environment.

30 x 30 mm square samples were prepared for the biodegradability test. The weight loss of samples placed on an open ground with soil and grass was determined. The samples were regularly turned (surface facing the sun and the other facing the ground) in the morning after every 2 days. The samples were collected from the open field after respectively 5, 12, 19, 26, 33, 40 and 47 days, washed with 100 mL acetone for 5 minutes and dried in a vacuum oven for 16 hours at 50 °C. The weight loss w_{loss} (%) was calculated using Equation 3.2.

$$w_{loss} = \frac{w_{initial} - w_{final}}{w_{final}} \times 100\% \quad (3.2)$$

Where $w_{initial}$ and w_{final} are the weights of specimens measured before and after placing the sample in the open environment with soil and grass [6-9].

3.3.6 Scanning electron microscopy (SEM)

The scanning electron microscope images the sample surface by scanning it with a high-energy beam of electrons in a raster scan pattern. The electrons interact with the atoms that make up the sample, producing signals that contain information about the sample's surface topography, composition and other properties such as electrical conductivity. In SEM the nature of the sample determines the preparation of the sample, since appropriate samples may be examined directly with little or no prior preparation. Unfortunately, most polymers present specific problems making them inappropriate. Therefore proper sample preparation is necessary prior to characterization, and these include (i) plasma etching, (ii) conductive coatings through evaporation or sputtering; and (iii) chemical etching methods [1].

The morphology of the samples was investigated with a Shimadzu SSX-550 superscan scanning electron microscope. The pictures were taken at room temperature. A field emission gun and an accelerating voltage of 5 kV was used. The fracture surfaces of the samples were coated with gold and the samples were viewed perpendicular to the fracture surfaces.

3.3.7 Fourier-transform infrared (FTIR) spectroscopy

Fourier-transform infrared spectroscopy is a technique for identifying types of chemical bonds in a molecule by producing an infrared absorption spectrum that is like a molecular "fingerprint". The chemical bonds can be either organic or inorganic, and it can give important information about the structure of organic molecules. It can be utilized to identify compounds and investigate sample composition, as well as interactions/reactions between functional groups on the different components in polymer blends and composites. [10,11].

FTIR spectroscopy was performed using a Perkin Elmer Spectrum 100 infrared spectrometer. The unmodified and modified fibre and copolyester/kenaf fibre composites were analysed in

an attenuated total reflectance (ATR) detector over a 400-4000 cm^{-1} wavenumber range at a resolution of 4 cm^{-1}.

3.3.8 Gel content determination

Gel content analysis is a technique to determine the extent of crosslinking or grafting in the composites. The gel in a crosslinked polyolefin can be determined by solvent extraction with solvents such as toluene or xylene.

The gel content of the composites was determined through xylene extraction of the uncross-linked parts of the sample. Small samples of 10 x 10 mm were weighed and wrapped in fine stainless steel mesh with aperture sizes varying from 0.50 to 0.90 μm. The wrapped samples were tied with a string and then placed in a round-bottomed flask half filled with 50 ml of xylene and refluxed for 16 hours. The samples were suspended just above the level of xylene throughout the experimental period. The solvent was changed after 8 hours of extraction. After the extraction, the wrapped samples were air-dried at ambient temperature for 24 hours and then dried at 50 °C in a vacuum oven for 24 hours. The gel content was determined using the following equations.

$$W_{extracted} = W_{(sample+mesh)be} - W_{(sample+mesh)ae} \quad (3.3)$$

$$W_{polymer} = W_{sample} \times 0.9 \quad (3.4)$$

$$\% \text{ Extraction} = \frac{W_{extracted}}{W_{polymer}} \times 100\% \quad (3.5)$$

$$\% \text{ Gel} = 100 - \% \text{ Extraction} \quad (3.6)$$

where $w_{extracted}$ is the extracted weight, w_{sample} is the weight composite, $w_{(sample+mesh)\ be}$ and $w_{(sample+mesh)\ ea}$ are the weight of the composite and the mesh before and after extraction and $w_{polymer}$ is the weight of polymer without fibre.

3.4 References

1. B.J. Hunt, M.I. James. Polymer Characterization, 1st edition. Blackie Academic & Professional, London (1997).
2. E.M. Pearce, C.E. Wright, B.K. Bordoloi. Laboratory Experiments in Polymer Synthesis and Characterization. The Pennsylvania State University, University Park, PA (1982).
3. E.L. Charsley, S.B. Warrington. Thermal Analysis – Techniques and Applications, Royal Society of Chemistry, Leeds (1992).
   ISBN: 0-85186-375-2
4. C.W. Shyang. Tensile and thermal properties of poly(butylene terephtalate)/organo-montmorillonite nanocomposites. Malaysian Polymer Journal 2008; 3:1-13.
5. M.E. Brown. Introduction to thermal analysis: Techniques and Applications. Chapman & Hall, London (1988).
   ISBN: 0 412 30230 6
6. M. Itävaara, M. Vikaman. An overview of methods for biodegradability testing of biopolymers and packaging materials. Journal of Polymers and the Environment 1996; 4:29-36.
   DOI: 10.1007/BF02083880
7. http://sundoc.bibliothek.uni-halle.de/diss-online/02/02H017/t7.pdf
8. http://en.wikipedia.org/wiki/Biodegradation
9. L. Liu, J. Yu, X. Yang. Biodegradability of poly(butylene succinate) (PBS) composite reinforced with jute fibre. Polymer Degradation and Stability 2009; 94:90-94.
   DOI: 10.1016/j.polymdegradstab.2008.10.013
10. http://en.wikipedia.org/wiki/FTIR
11. D.L. Pavia, G.M. Lampman, G.S. Kriz Jr. Introduction to Spectroscopy: A Guide for Students of Organic Chemistry. Harcourt Brace Jovanovich College, Orlands (1979).
    ISBN: 0-7216-7119-5

CHAPTER FOUR

RESULTS AND DISCUSSION

4.1 Scanning electron microscopy (SEM)

The SEM micrographs of the fractured surfaces of untreated and treated copolyester/kenaf fibre composites at 10% kenaf content are illustrated in Figures 4.1 to 4.4. For each sample two magnifications were used to display both the fibre dispersion and interfacial adhesion. The untreated composite shows a large number of holes or voids (Figure 4.1(a), arrow A) in the CP matrix resulting from fibre pullouts. There is also no evidence of fibre fracture. There are also distinct gaps between the fibres and the matrix (Figure 4.1(b), arrow C), which may be related to the debonding between them. It can be further seen that there is agglomeration of fibres in the CP matrix (Figure 4.1(a), arrow B). Liu *et al.* [1] investigated the influence of fibre treatment of Indian grass fibre on the properties of biocomposites derived from grass fibre and soy based bioplastic. For the untreated fibre a similar large number of holes or voids resulting from extensive fibre pullout were observed. This observation was related to the poor interfacial adhesion between the soy based bioplastic and the grass fibre. This was probably caused by the hemicellulose/lignin mixture in the fibre that reduces the interaction between the fibre and matrix. This is also in agreement with observations by other authors [2-5].

For the alkali treated composites (Figure 4.1(c)) there is evidence of fibre and matrix interaction (Figure 4.1d), and the matrix comprises of fewer voids from fibre pullout compared to the untreated composites (Figures 4.1(a) and 4.1(b)). The interaction is probably as a consequence of the alkali treatment introduced to the kenaf fibre resulting in a rough surface allowing the polymer to adhere to the fibre through mechanical interlocking [6,7].

Figure 4.2 represents the micrographs of CP/NaOH-kenaf, where the fibre was modified with a silane coupling agent at various concentrations. The introduction of 3% silane to the fibre (Figure 4.2(a)) gave rise to fewer fibre pullouts compared to the untreated composites (Figure 4.1(a)). There are also no gaps or voids visible between the matrix and the fibre (Figure 4.2(b)). This is probably due to better compatibility between the fibre and the matrix. The introduction of coupling agents or compatibilizers commonly brings about crosslinking or grafting of the fibre to the matrix [4,6,8-10]. Furthermore, the fibres embedded in the matrix

show breakage on their surface (Figure 4.2(b), arrow A) after fracture of the composite. At higher silane concentrations better interaction can be clearly observed (Figure 4.2(c), 4.2(d), 4.2(e) and 4.2(f)). Figures 4.2(d) and 4.2(f) show evidence of broken fibre ends embedded in the matrix. This clearly indicates that the adhesion between the fibre and the matrix was improved. The same behaviour was observed by Pothan *et al.* [11]. The author investigated the effect of fibre surface treatments on the fibre-matrix interaction in banana fibre reinforced polyester composites. The silane modified fibre composites similarly indicated evidence of broken fibre and no fibre pullouts. The improved adhesion of the composite is due to the ability of the silanol coupling agent to react with the −OH group in the fibre, forming stable covalent bonds, which create a crosslinking network between the matrix and the fibre.

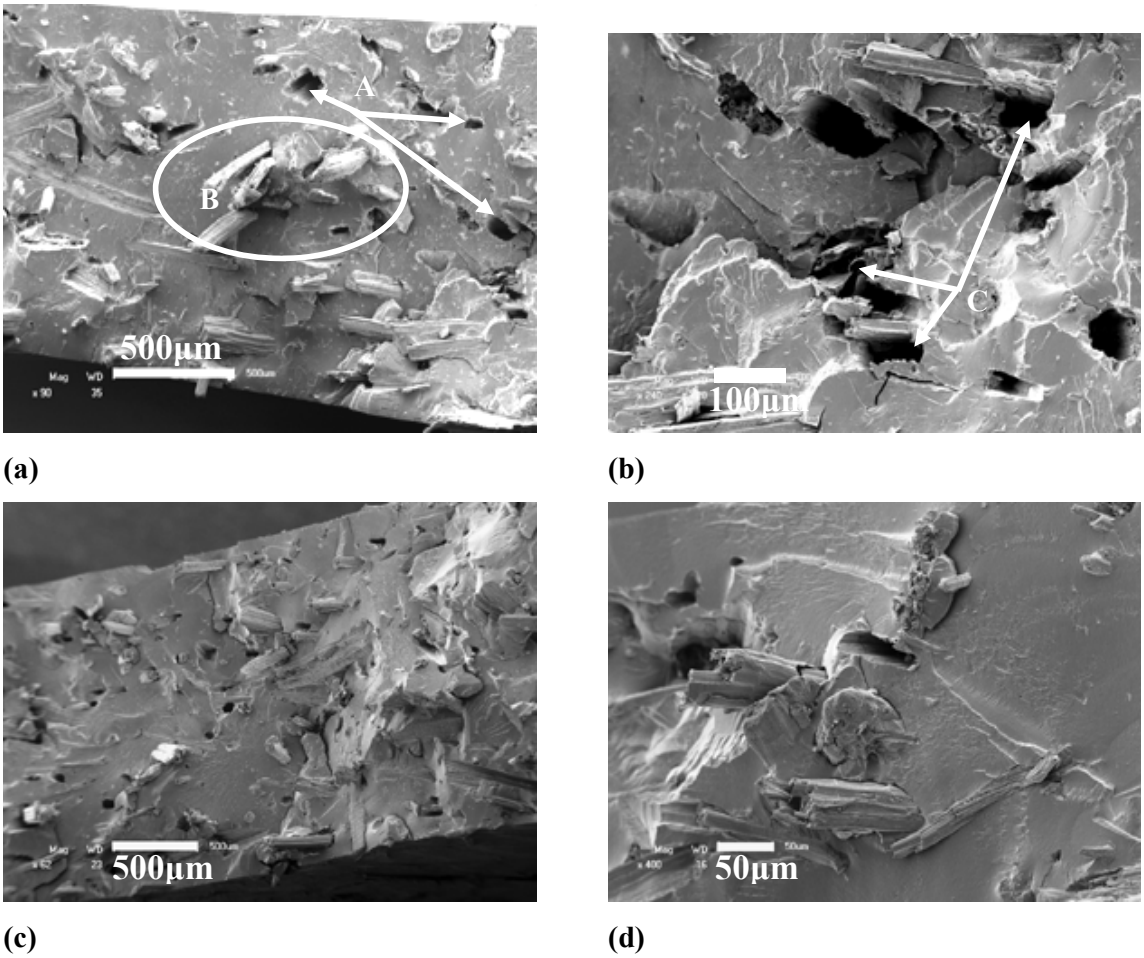

(a) **(b)**

(c) **(d)**

Figure 4.1 SEM images for 90/10 w/w CP/Kenaf ((a) 35x magnification and (b) 240x magnification) and 90/10 w/w CP/NaOH-Kenaf ((c) 62x magnification and (d) 400x magnification)

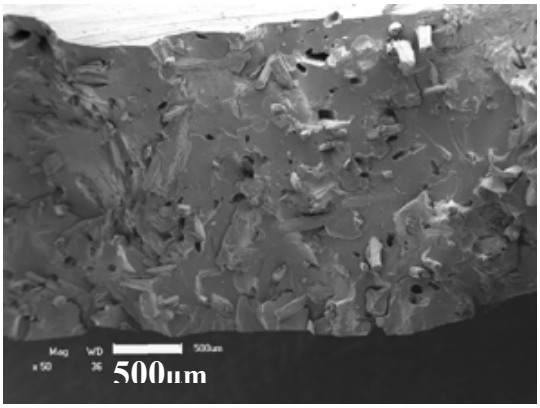

(a)

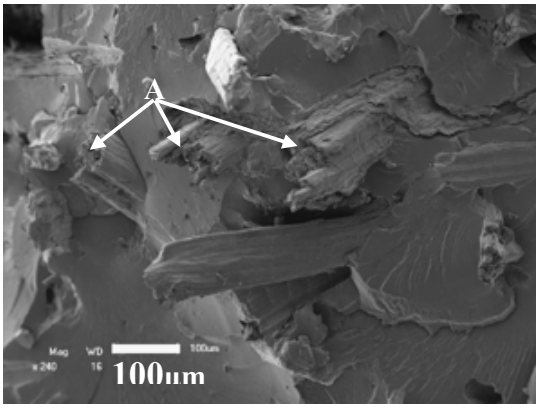

(b)

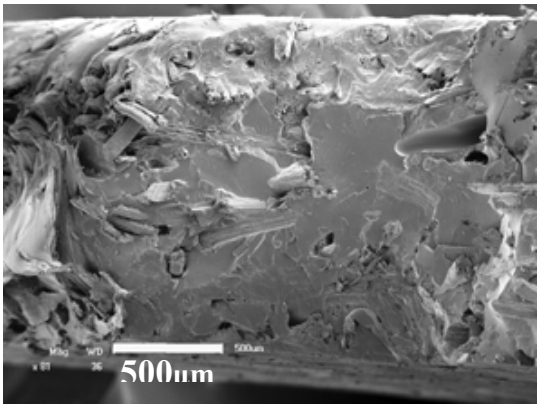

(c)

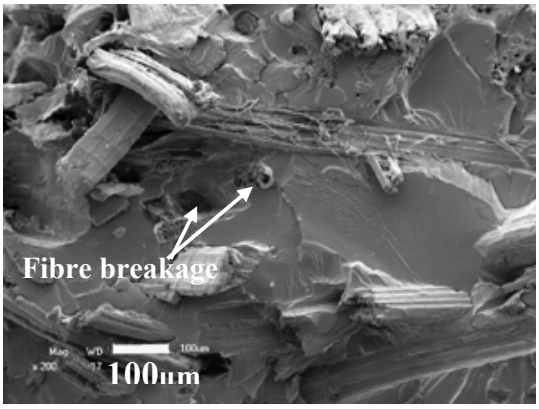

(d)

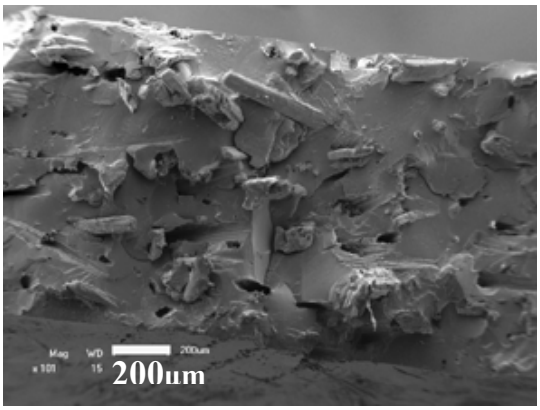

(e)

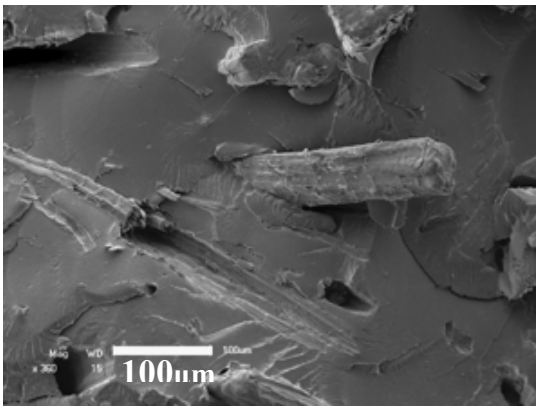

(f)

Figure 4.2 SEM micrographs for 90/10 w/w CP/NaOH-Kenaf-silane3 ((a) 50x magnification and (b) 240x magnification), 90/10 w/w CP/ NaOH-Kenaf-silane6 ((c) 61x magnification and (d) 200x magnification), and 90/10 w/w CP/NaOH-Kenaf-silane9 ((e) 101x magnification and (f) 360x magnification)

Figures 4.3 and 4.4 represent the micrographs of CP/NaOH-kenaf where the fibre was modified with Disperal nanofiller at various concentrations. The Disperal treated fibre composites also show interaction between the fibre and the matrix, because there are still fibres embedded in the matrix after sample fracture (Figure 4.3(b), 4.3(d), 4.4(b), 4.4(d)). The CP/NaOH-kenaf-silane-Disperal10 (Figure 4.4(d)) shows no fibre pullouts, but the composites show (i) twisting or bending of the fibre in the matrix and (ii) the fibre observed are fully covered and buried in the matrix.

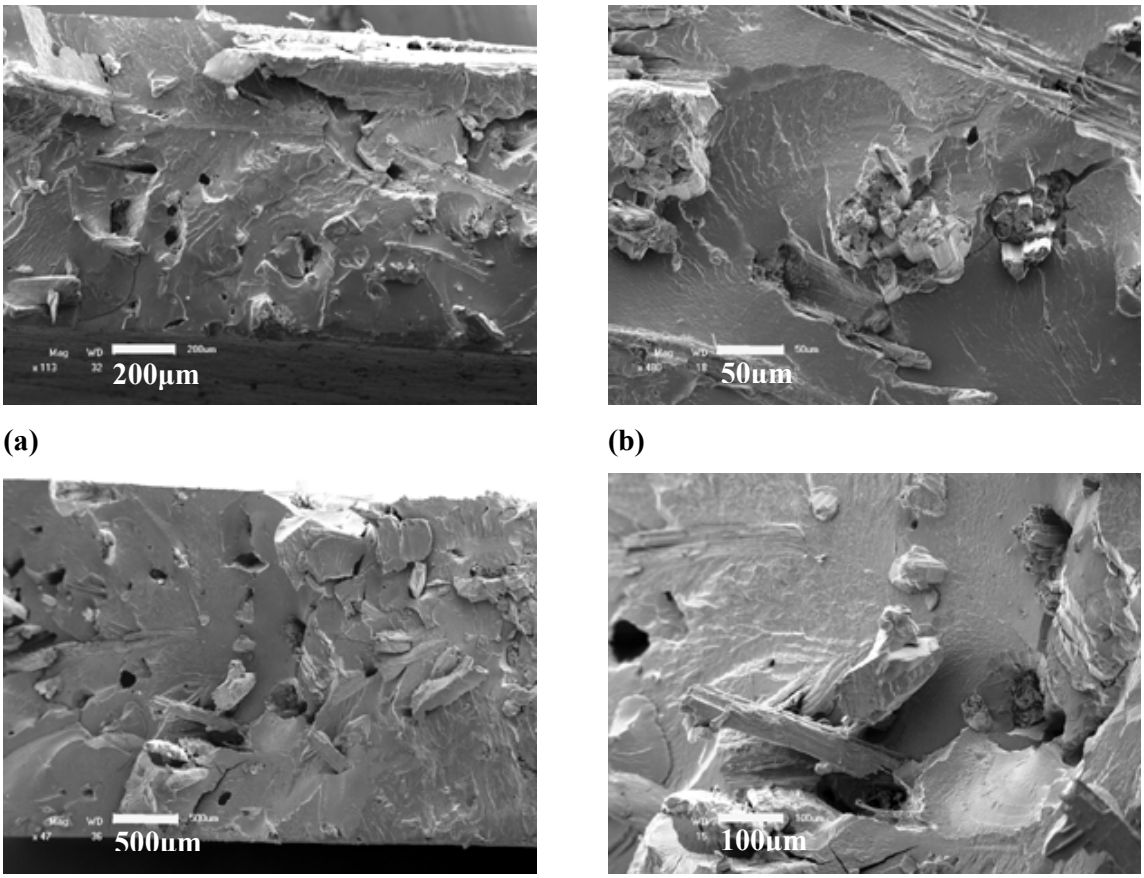

(a) **(b)**

(c) **(d)**

Figure 4.3 SEM micrographs for 90/10 w/w CP/NaOH-kenaf-silane3-Disperal4 ((a) 113x magnification and (b) 480x magnification) and 90/10 w/w CP/NaOH-kenaf-silane3-Disperal6 ((c) 47x magnification and (d) 240x magnification)

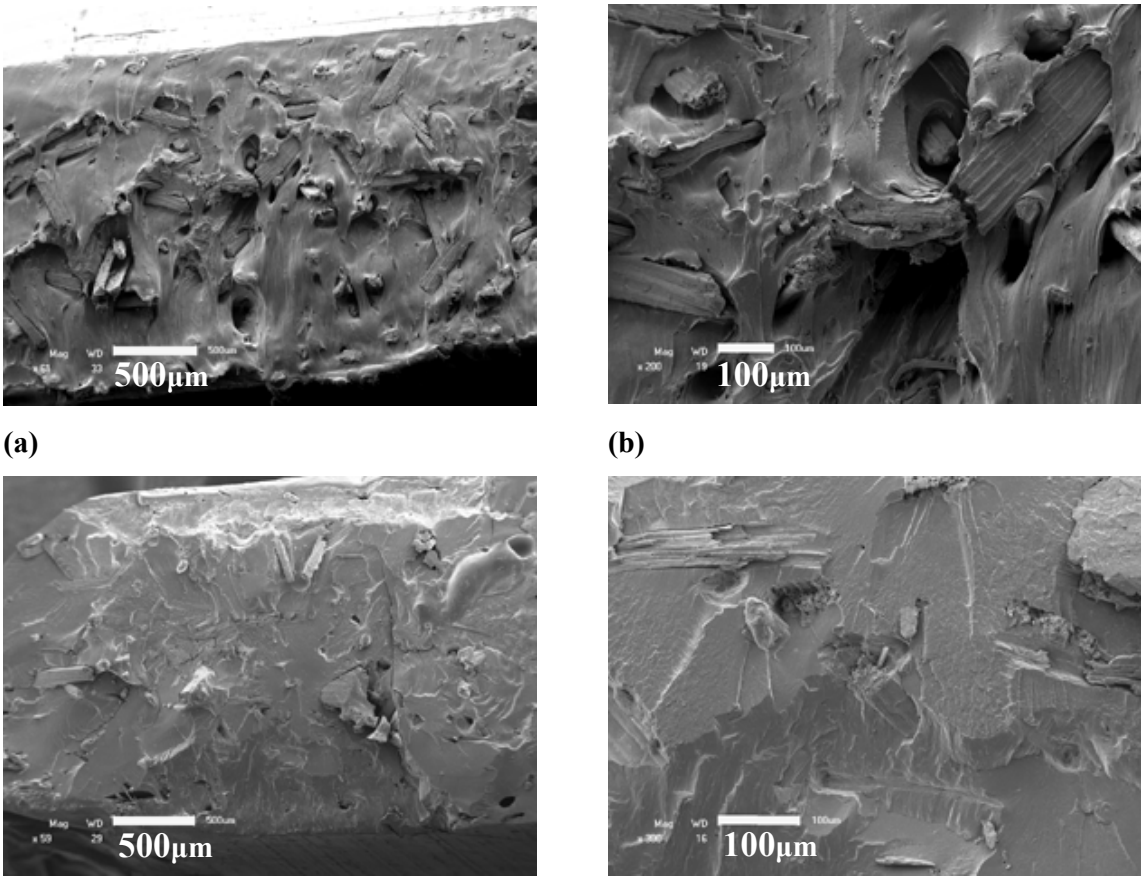

(a) **(b)**

(c) **(d)**

Figure 4.4 SEM micrographs for 90/10 w/w CP/NaOH-Kenaf-silane3-Disperal8 ((a) 113x magnification and (b) 480x magnification) and 90/10 w/w CP/NaOH-Kenaf-silane3-Disperal10 ((c) 47x magnification and (d) 240x magnification)

4.2 Attenuated total reflectance Fourier-transform infrared (ATR-FTIR) spectroscopy

The ATR-FTIR spectra of kenaf and NaOH-kenaf fibres are shown in Figure 4.5, while Figure 4.6 shows the spectra for CP, CP/NaOH-kenaf, CP/NaOH-kenaf-silane9 and CP/NaOH-kenaf-silane3-Disperal10. Some band assignments are listed in Table 4.1.

The spectra of kenaf and NaOH-kenaf in Figure 4.5 are dominated by the peaks at 3200-3400 cm^{-1} and 1000-1100 cm^{-1}, that are respectively due to the stretching vibrations of O-H and C-O-C. A broad absorption band in the region 3200-3400 cm^{-1}, as well as the characteristic hydrogen bonded –OH stretching vibration, can both be found in the FTIR spectra of kenaf

fibre, whether treated or not. However, after the removal of hemicellulose, the α-cellulose fraction is expected to increase [12]. However, there is not much of a difference between the O-H stretching peak intensities of the unmodified and NaOH modified fibre. Since the presence of water may also contribute to the intensity of this peak, it is difficult to see from this peak what influence the NaOH treatment had on the fibre structure and composition. The peak at 1000-1100 cm^{-1} belongs to the C-O-C stretching of lignin. The kenaf fibre shows a peak at 1740 cm^{-1} assigned to C=O, which disappeared when the fibres were treated with the NaOH aqueous solution. The observation shows the removal of hemicellulose by alkali treatment. The vibrational peak around 2900 cm^{-1}, belonging to the C—H stretching vibration in cellulose and hemicelluloses, decreased after NaOH treatment. It indicates that part of the hemicellulose was removed [1]. Furthermore, the peak around 1633 cm^{-1} for C-O assigned to the ester and ether cross-link between cellulose and lignin, or cellulose and hemicelluloses, disappeared during NaOH treatment. This is due to the removal of acid, lignin and other fibre constituents as observed by Lai *et al.* [13] in their investigation of the properties of woven kenaf and betel palm reinforced unsaturated polyester composites. The intense peak at 1000-1162 is assigned to C-C stretching.

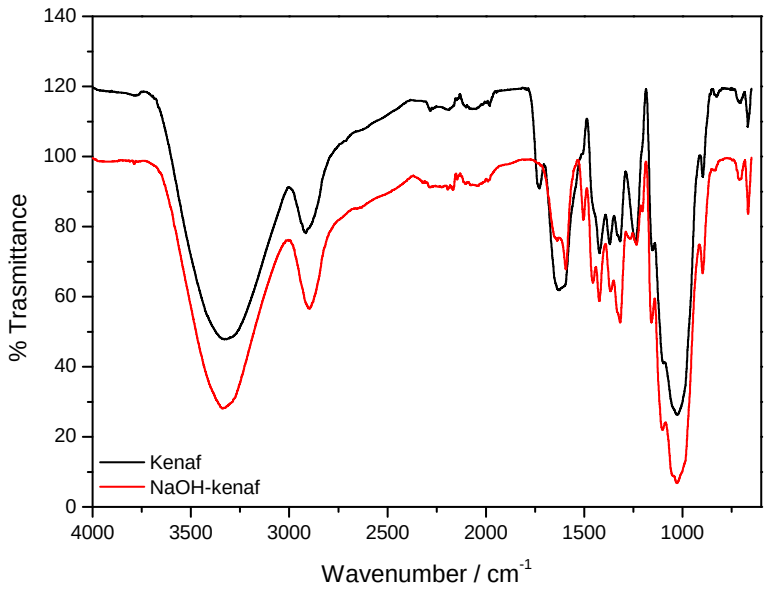

Figure 4.5 FTIR spectra of kenaf and NaOH-kenaf fibre

The CP/NaOH-kenaf composite shows the same broad intense peak, which was observed for the NaOH-kenaf, at 3200-3400 cm^{-1} (Figure 4.6). This peak is due to the –OH groups in the fibre. Reduced peak intensity was observed for the CP/NaOH-kenaf-silane9 composite due to the ability of the silanols in the coupling agent to react with the -OH group in the fibre, forming stable covalent bonds [1,11-14]. The two peaks at 3280 and 3094 cm^{-1} observed for the Disperal containing composites are assigned to the -OH asymmetric and symmetric stretching vibrations. These two clearly defined peaks that are also observed for neat Disperal clearly overshadow the broad –OH peak normally observed in the same wavenumber range.

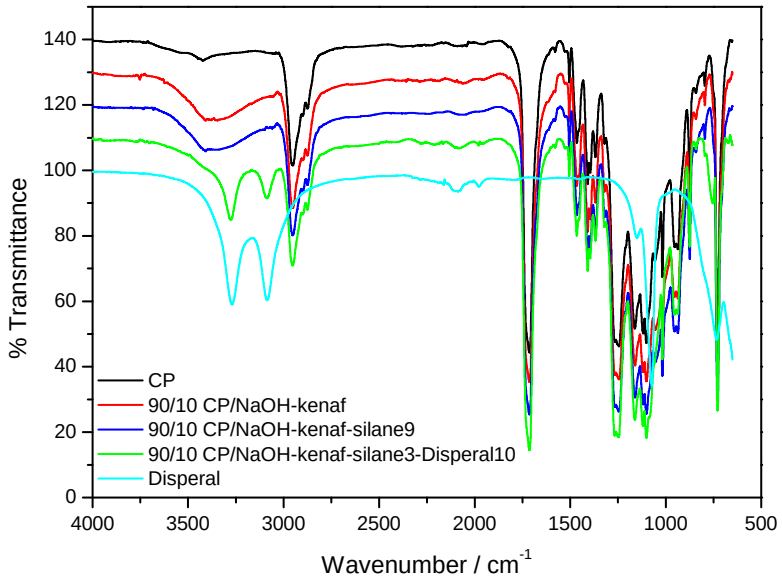

Figure 4.6 FTIR spectra of CP, CP/NaOH-kenaf, CP/NaOH-kenaf-silane9 and CP/NaOH-kenaf-silane3-Disperal10

The intense peak at 1700-1750 cm^{-1} is assigned to the C=O stretching in unconjugated ketones and carbonyl groups in the CP polymer chains. The CP/NaOH-kenaf-silane9 spectrum shows the stretching bands of –Si—O—C– and –Si—O—Si– around 1020-1080 cm^{-1} and 1188-1189. The–Si—O—C– peak indicates that hydrolysis and condensation reactions between silane and the kenaf fibre have occurred. The presence of the siloxane –Si-O-Si– peak shows that silane was absorbed by the fibre surface, as also observed by He *et al* [15]. The author investigated the effect of silane coupling agents on the interfacial properties of carbon fibre-polyamide composites. The presence of the Disperal nano-powder in the CP/NaOH-kenaf-silane3-Disperal10 composite gives rise to strong peaks at 698, 737, 810 and 998 cm^{-1}, that

indicate the asymmetric stretching, angle bending and angle deformation (wagging) of (OH)-Al=O [16,17]. The sharp peak at 1430 cm^{-1} may be from the vibration overtone of surface –OH groups [16]. The vibrations observed at 1000-1310 cm^{-1} may be due to the overlapping of Al—O—Si–, –Si—O—Si– and C—O—Si– from the silane and Disperal [18,19].

Table 4.1 some important peaks in the FTIR spectra of kenaf, CP, CP/NaOH-kenaf, CP/NaOH-kenaf-silane9 and CP/NaOH-kenaf-silane3-Disperal10

Wavenumber / cm^{-1}	Assigned vibrations	Visible in
698, 737, 810 and 998	asymmetric stretching, angle bending and angle deformation of (OH)–Al=O	CP/NaOH-kenaf-silane3-Disperal10
1000-1310	overlapping of Al—O—Si–, Si—O—Si– and C—O—Si–	CP/NaOH-kenaf-silane3-Disperal10
1020-1080	stretching bands of –Si—O—C	CP/NaOH-kenaf-silane9
1000-1100	C—O stretching	Kenaf, NaOH-kenaf and CP/NaOH-kenaf
1188-1189	stretching bands of –Si—O—Si–	CP/NaOH-kenaf-silane9
1430	the vibration overtone of surface –OH groups	CP/NaOH-kenaf-silane3-Disperal10
1633	C—O	Kenaf
1740	C=O disappears	Kenaf
1700-1750	C=O stretching	All composites
2900	C—H	Kenaf and NaOH-kenaf
3075 and 3270	stretching vibration of –OH	CP/NaOH-kenaf-silane3-Disperal10 and Disperal
3200-3400	stretching vibrations of –OH	Kenaf, NaOH-Kenaf and CP/NaOH-kenaf

4.3 Differential scanning calorimetry (DSC)

The DSC heating curves for the copolyester/kenaf fibre composites are summarized in Figures 4.7 and 4.8, while Figures 4.9 and 4.10 show the cooling curves. The peak temperatures of melting and crystallization, as well as the melting and crystallization enthalpies, of all the samples are shown in Tables 4.2 and 4.3. All the reported DSC heating and cooling results were obtained from the second scan to eliminate the effect of thermal history. The calculated melting enthalpy (ΔH_m^{cal}) was calculated from the experimentally observed melting enthalpy (ΔH_m^{obs})$_{CP}$ of the neat copolyester (CP) and the weight fraction of the polymer (W_{CP}) according to Equation 4.1.

$$\Delta H_m^{cal} = (\Delta H_m^{obs})_{CP} \times W_{CP} \qquad (4.1)$$

Figure 4.7 represents the DSC curves for the CP/kenaf fibre composites, where the fibre was modified with silane at different concentrations. CP and its composites show very broad melting peaks and the peaks seem to slightly shift to higher temperatures for the silane treated fibre composites. The most probable reason for this is that silane initiated grafting between the fibre and the polymer caused epitaxial crystallization and crystal growth on the fibre surfaces which may have influenced the crystallization and melting behaviour of the polymer. The interaction between the alkali and silane treated fibre and the matrix should be much stronger than that the fibres treated with alkali alone. This is because NaOH treatment normally only roughens the fibre surface so that there may be a better physical interaction through mechanical interlocking, whereas silane treatment should initiate grafting between the fibre and the matrix.

The melting and crystallization enthalpy values are observably scattered, and there is no real trend with increasing silane or Disperal contents (Tables 4.2 and 4.3). It does; however, seem as if the values for the composites are slightly lower than that of pure CP, indicating some immobilization effect of the fibre on the polymer chains.

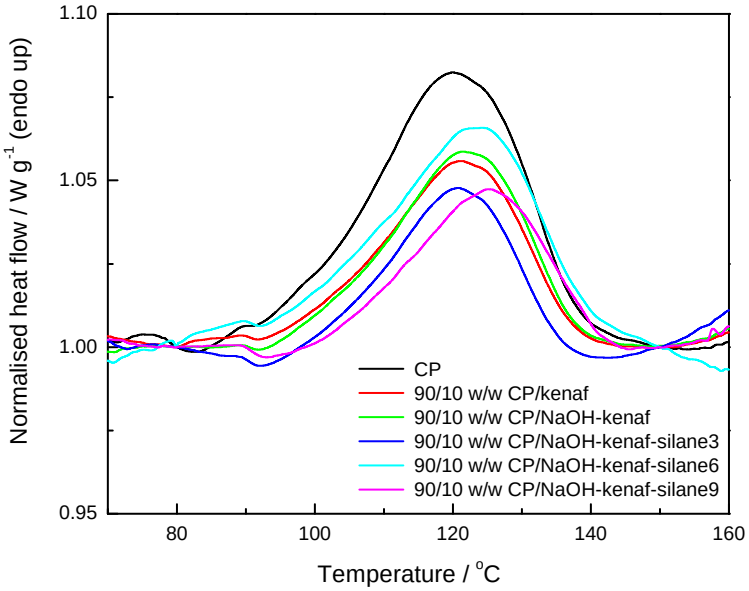

Figure 4.7 DSC heating curves for the samples prepared in the absence of Disperal

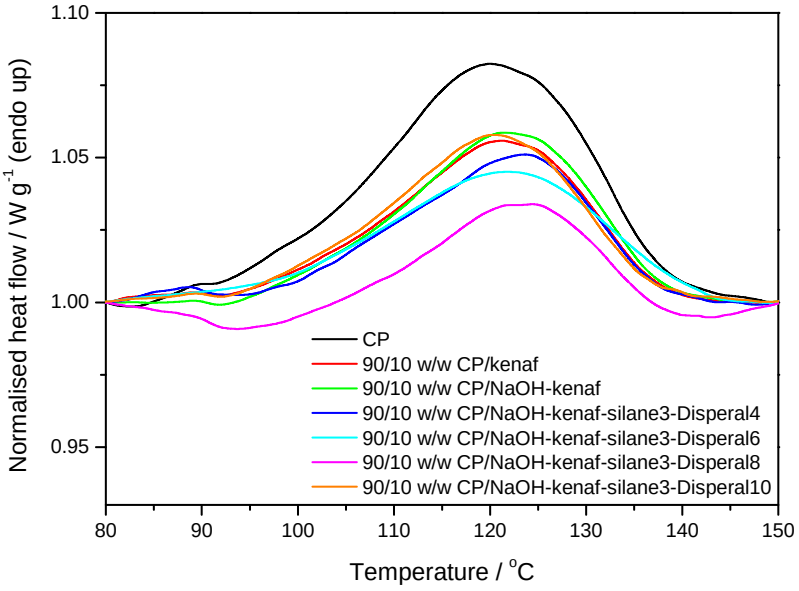

Figure 4.8 DSC heating curves for the samples prepared in the presence of Disperal

Figure 4.8 shows the curves of the CP/NaOH-kenaf-silane3 composites where the fibres were treated with Disperal nano-powder. The melting and crystallization enthalpies of these composites (i) are scattered and show no trend, and (ii) have the same order of magnitude than the calculated enthalpy values. Furthermore, the 4% and 10% Disperal containing composites have melting peak temperatures that are the same as that for CP/NaOH-kenaf/silane3, while the 6% and 8% Disperal containing composites have observably higher values, but again no trend was observed. The crystallization temperatures also show no trend, and it seems as if within experimental error the Disperal has almost no influence on the melting and crystallization behaviour of the polymer.

Table 4.2 Summary of DSC heating data for the copolyester/kenaf fibre composites

Composites (w/w)	$T_{p,m}$ / °C	ΔH_m^{obs} / J g^{-1}	ΔH_m^{cal} / J g^{-1}
100/0 CP	121.8 ± 0.7	9.6 ± 1.1	9.6
90/10 CP/kenaf	120.9 ± 0.2	8.0 ± 0.4	8.6
90/10 CP/NaOH-kenaf	120.7 ± 0.7	8.1 ± 1.1	8.6
90/10 CP/NaOH-kenaf-silane3	121.5 ± 0.8	7.3 ± 1.3	8.6
90/10 CP/NaOH-kenaf-silane6	122.8 ± 1.1	10.3 ± 1.2	8.6
90/10 CP/NaOH-kenaf-silane9	125.8 ± 0.9	6.6 ± 0.4	8.6
90/10 CP/NaOH-kenaf-silane3-Disperal4	121.5 ± 0.2	7.3 ± 1.7	8.6
90/10 CP/NaOH-kenaf-silane3-Disperal6	124.6 ± 0.5	10.0 ± 0.7	8.6
90/10 CP/NaOH-kenaf-silane3-Disperal8	124.7 ± 0.6	8.5 ± 0.6	8.6
90/10 CP/NaOH-kenaf-silane3-Disperal10	120.7 ± 0.6	9.5 ± 1.6	8.6

$T_{p,m}$, ΔH_m^{obs}, ΔH_m^{cal}, are respectively the peak temperature of melting, observed melting enthalpy, and calculated melting enthalpy

Table 4.3 Summary of DSC cooling data for the copolyester/kenaf fibre composites

Composites (w/w)	$T_{p,c}$ / °C	ΔH_c^{obs} / J g^{-1}	ΔH_c^{cal} / J g^{-1}
100/0 CP	73.4 ± 0.7	-15.8 ± 0.9	-15.8
90/10 CP/kenaf	79.1 ± 0.2	-15.4 ± 1.4	-14.2
90/10 CP/NaOH-kenaf	78.7 ± 0.3	-12.6 ± 0.5	-14.2
90/10 CP/NaOH-kenaf-silane3	81.1 ± 0.6	-13.0 ± 1.7	-14.2
90/10 CP/NaOH-kenaf-silane6	82.4 ± 1.0	-11.6 ± 0.7	-14.2
90/10 CP/NaOH-kenaf-silane9	84.9 ± 0.3	-12.6 ± 0.4	-14.2
90/10 CP/NaOH-kenaf-silane3-Disperal4	84.1 ± 0.7	-11.3 ± 0.1	-14.2
90/10 CP/NaOH-kenaf-silane3-Disperal6	86.1 ± 0.7	-12.4 ± 1.0	-14.2
90/10 CP/NaOH-kenaf-silane3-Disperal8	81.4 ± 1.2	-13.5 ± 0.4	-14.2
90/10 CP/NaOH-kenaf-silane3-Disperal10	80.7 ± 1.0	-11.7 ± 0.7	-14.2

$T_{p,c}$, ΔH_c^{obs}, ΔH_c^{cal} are respectively the peak temperature of crystallization, the observed crystallization enthalpy, and the calculated crystallization enthalpy

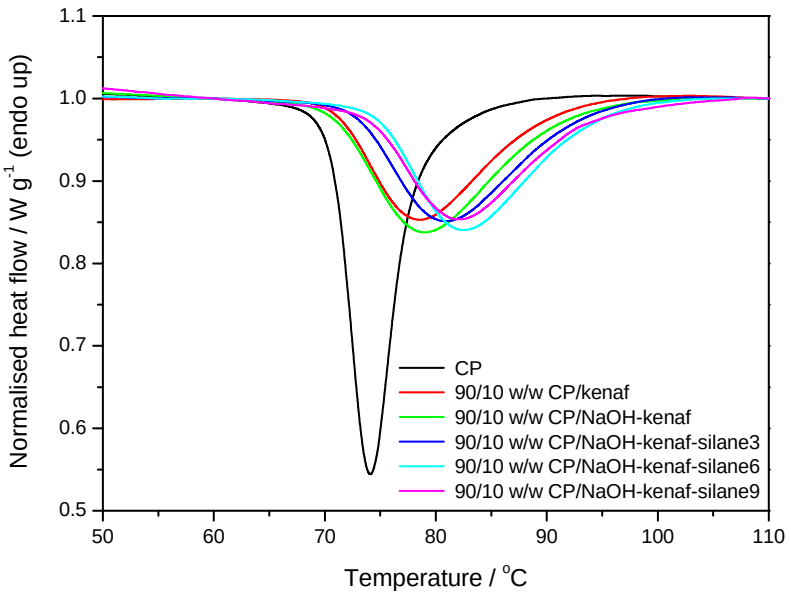

Figure 4.9 DSC cooling curves for the samples prepared in the absence of Disperal

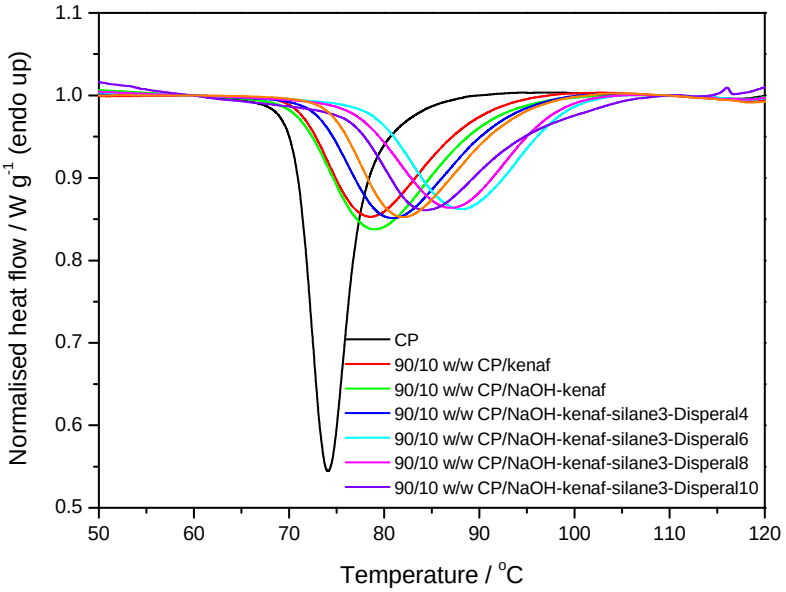

Figure 4.10 DSC cooling curves for the samples prepared in the presence of Disperal

4.4 Thermogravimetric analysis (TGA)

The TGA results of all the samples are shown in Figures 4.11 and 4.12. Their thermal stabilities were characterized in terms of the temperatures at 10 and 50% mass loss (Table 4.4). The TGA curves in Figure 4.11 shows one-step degradation for the CP/kenaf fibre composites, while the kenaf fibre shows more than one degradation step. The first step below 100 °C for kenaf fibre is due to the vaporization of moisture. The second step around 253 °C is due to the thermal depolymerisation of hemicellulose and the cleavage of glycosidic linkages of cellulose. The third step above 360 °C is due to the decomposition of cellulose. The composites show degradation below 100 °C, which can be associated with loss of moisture from the fibre. The CP matrix is thermal stable up to 300 °C (Figure 4.11) and decomposes with the formation of about 4% char. The composites started degrading at lower temperatures than CP (see $T_{10\%}$ in Table 4.4). This is the result of the presence of kenaf fibre which degrades at lower temperatures. However, the main decomposition (see $T_{50\%}$ in Table 4.4) occurs at slightly higher temperatures for all the composites, and the residues at 650 °C are higher than that of neat CP (Figure 4.11). The degradation of the polymer backbone in the CP/NaOH-kenaf sample occurs at a higher temperature than the other samples. This is

probably because the alkali treatment brings about an increased surface roughness in the fibre which results in better mechanical interlocking between the filler and the matrix. As a result the fibre may retard the movement of free radicals formed during the initiation of degradation, or it may interact with volatile degradation products and in the process slow down their diffusion out of the sample.

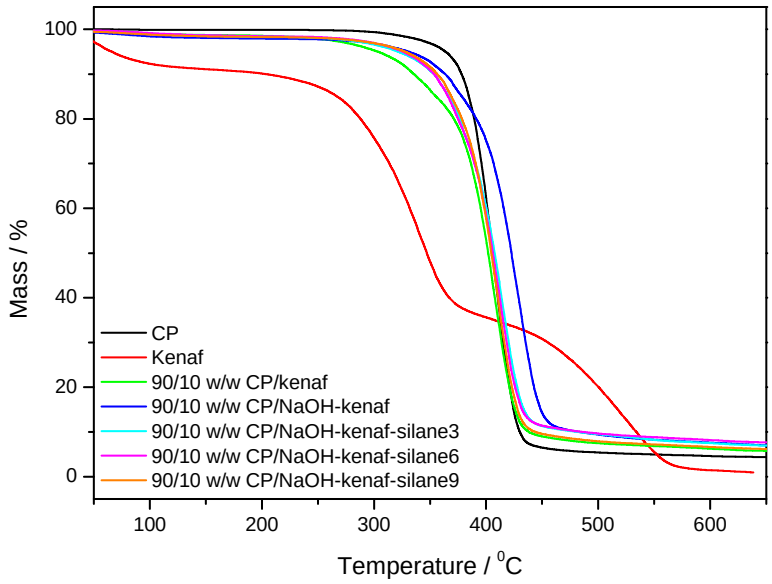

Figure 4.11 TGA curves for the samples prepared in the absence of Disperal

Figure 4.12 shows the TGA curves of the Disperal containing composites. Generally the presence of Disperal seems to increase the thermal stability of the composites (Table 4.4). Possible reasons for this are (i) that the Disperal nanofiller may preferably absorb the heat and as a result retard the decomposition process, or (ii) that it could possibly interact with the volatile decomposition products and in the process retard its diffusion out of the sample.

Table 4.4 Summary of the TGA results for the copolyester/kenaf fibre composites

Sample w/w	$T_{10\%}$ / ^{o}C	$T_{50\%}$ / ^{o}C
CP	377.2	405.9
Kenaf	183.2	346.8
90/10 CP/kenaf	334.2	400.2
90/10 CP/NaOH-kenaf	362.4	420.7
90/10 CP/NaOH-kenaf-silane3	351.2	407.1
90/10 CP/NaOH-kenaf-silane6	353.6	407.8
90/10 CP/NaOH-kenaf-silane9	355.7	405.5
90/10 CP/NaOH-kenaf-silane3-Disperal4	347.1	402.9
90/10 CP/NaOH-kenaf-silane3-Disperal6	349.8	406.6
90/10 CP/NaOH-kenaf-silane3-Disperal8	368.4	414.3
90/10 CP/NaOH-kenaf-silane3-Disperal10	361.0	406.7

$T_{10\%}$ and $T_{50\%}$ means temperatures at 10% and 50% weight loss

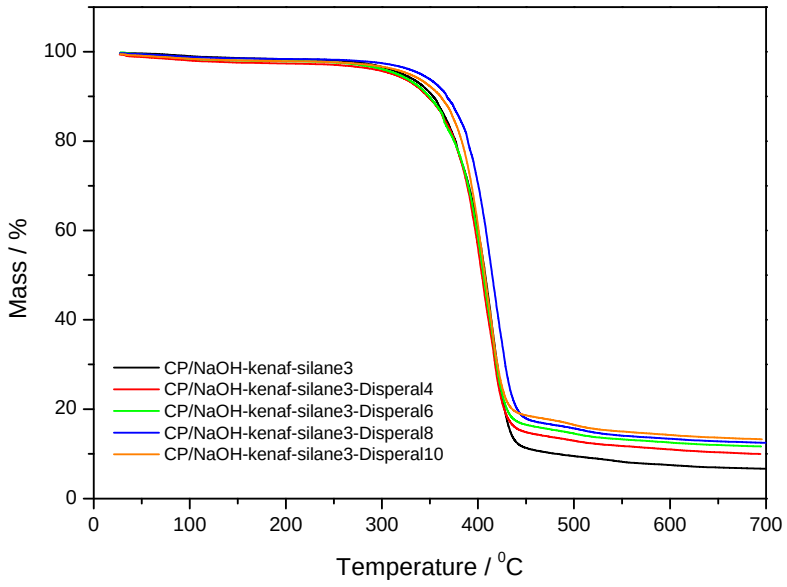

Figure 4.12 TGA curves for the samples prepared in the presence of Disperal

4.5 Dynamic mechanical analyses (DMA)

The effect of sodium hydroxide (NaOH), silane and Disperal treatments on the dynamic mechanical properties of copolyester/kenaf fibre composites are shown in Figures 4.13 to 4.18. The curves in Figure 4.13 indicate that below -40 °C the CP/kenaf shows higher moduli than pure CP, while the CP/NaOH-kenaf shows even higher moduli. All the silane treated composites show almost the same moduli in this temperature region, and their modulus values are between those of CP/kenaf and CP/NaOH-kenaf. The values for CP/kenaf are the result of the higher modulus of the fibre, while the higher values for CP/NaOH-kenaf are probably the result of an improvement in the surface roughness of the fibre as a result of NaOH treatment, which improves mechanical interlocking adhesion between CP and the fibre. Similar behaviour was observed in a study by Sharifah *et al.* [20] of the effect of alkalization and fibre alignment on the mechanical and thermal properties of kenaf fibre and hemp bast fibre composites with a polyester resin matrix. These observations are also in agreement with those by other authors [21,22]. The CP/NaOH-kenaf-silane (3%, 6% and 9%) composites show almost the same moduli over this temperature range, and their modulus values are lower than those of the CP/NaOH-kenaf composite. Although the differences in modulus in this temperature range are fairly small, the lower modulus of the silane treated samples may be attributed to the lowering of the fibre modulus by the impregnated silane. The storage modulus of the samples decreases with increasing temperature and a pronounced decrease is observed between -40°C and -30°C. This drop in modulus indicates the glass transition region of CP. All the composites show larger moduli than pure CP at temperatures above -30 °C, which might have been caused by the restriction in chain mobility caused by the interaction between the fibre and the polymer chains, especially for the samples where the fibres were modified. This is particularly obvious for the CP/NaOH-kenaf fibre composite, where the mechanical interlocking interaction significantly restricts the polymer chain mobility. The small transition at 40°C may be attributed to the crystalline region of the CP matrix, and is more clearly visible in the damping factor curves.

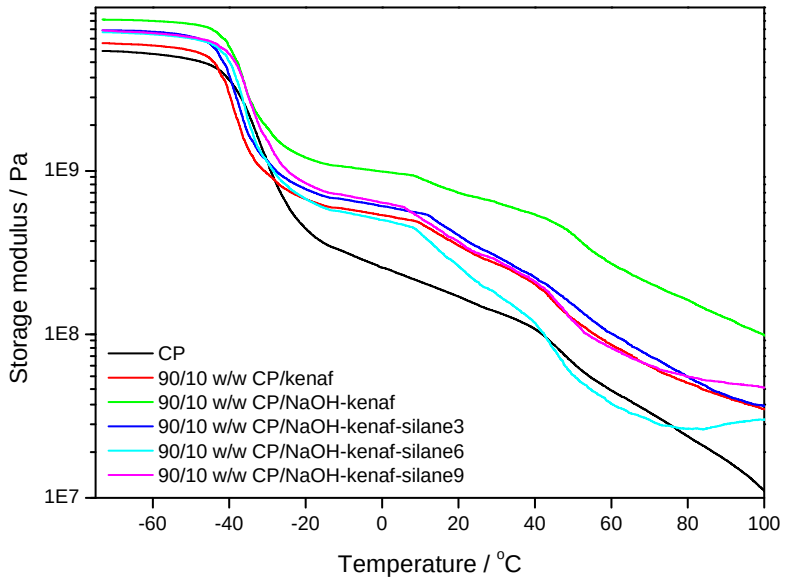

Figure 4.13 DMA storage modulus as function of temperature of CP, 90/10 w/w CP/kenaf, and the different silane treated composites

Figure 4.14 shows the storage modulus as function of temperature for the Disperal modified fibre composites. There is no clear trend in the influence of Disperal on the storage modulus values of the samples over the whole investigated temperature range, and it may be concluded that the presence and content of Disperal had very little influence on the storage moduli of CP/NaOH-kenaf-silane3.

Figure 4.15 shows the loss modulus (E") as function of temperature for CP and its composites. The neat CP shows a glass transition (T_g) around -30°C, whereas for the composites the T_g is slightly shifted to lower temperatures. There is no obvious reason for this observation, because interaction between the fibre and the polymer should immobilize the polymer chains and increase the glass transition temperature.

Figure 4.16 shows the loss modulus curves for the Disperal treated composites. As with the storage modulus curves, there is no specific trend with increasing Disperal content, and the modulus values are not significantly different. The CP/NaOH-kenaf-silane3-Dipseral10 shows a slight shift in the modulus to a lower temperature, which is probably a consequence of the plasticizing effect of Disperal on the CP matrix [23].

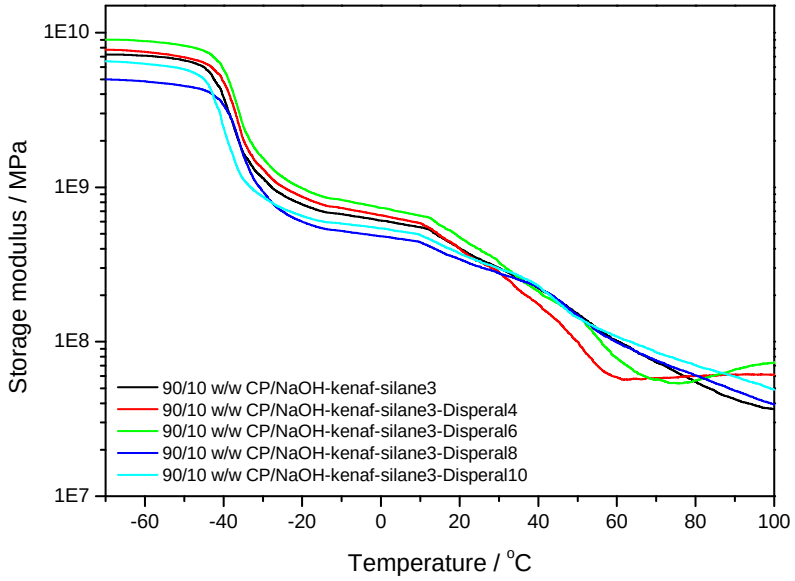

Figure 4.14 DMA storage modulus as function of temperature of CP/NaOH-kenaf-silane3, and CP/NaOH-kenaf-silane3-Disperal4, 6, 8 and 10 composites

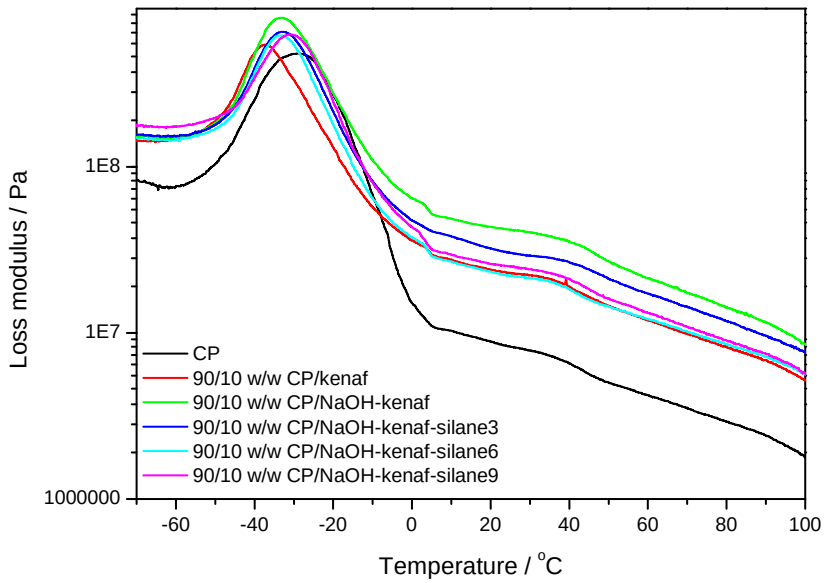

Figure 4.15 DMA loss modulus as function of temperature of CP, 90/10 w/w CP/kenaf, and the different silane treated composites

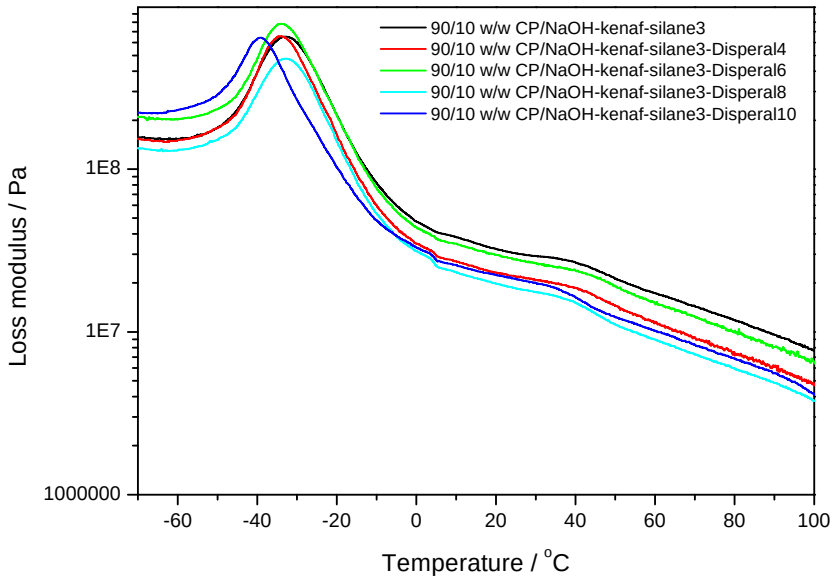

Figure 4.16 DMA loss modulus as function of temperature of CP/NaOH-kenaf-silane3, and the CP/NaOH-kenaf-silane3-Disperal composites

Figure 4.17 shows the damping factor (tan δ) as function of temperature for CP and its composites. The silane treated composites show two relaxation peaks, while the neat CP and the CP/NaOH-kenaf composite have only one relaxation peak. The damping peak observed between –20 and –30 °C for all the samples may be associated with the β- or glass transition of CP due to its semi-crystalline nature. The treated composites also show an α-transition between 70 and 90 °C associated with the molecular motion related to the crystalline phase. There is no relation between the position or intensity of this peak and the type of composite or composite treatment.

Figure 4.18 represents tan δ as function of temperature for the Disperal modified fibre composites. The Disperal modified composites show two transitions at low and high temperatures. The transitions are observed for the amorphous phase (β- or glass transition) at low temperatures and for the crystalline phase (α-transition) at higher temperatures. There is no trend in the position or intensity of both these transitions as a function of the presence of Disperal or its content, which makes it impossible to draw any conclusions on the influence of the presence of Disperal on the dynamic mechanical properties of these composites.

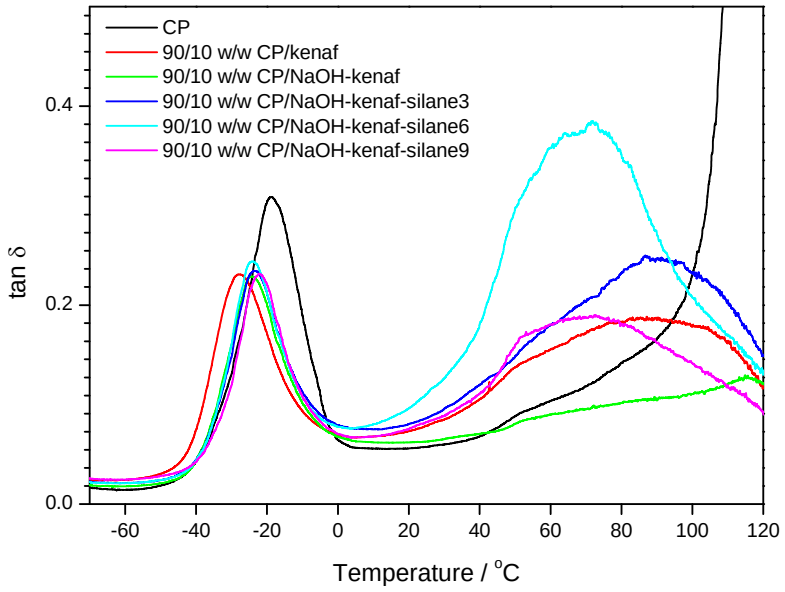

Figure 4.17 Damping factor (tan δ) as function of temperature of CP, 90/10 w/w CP/kenaf, and the different silane treated composites

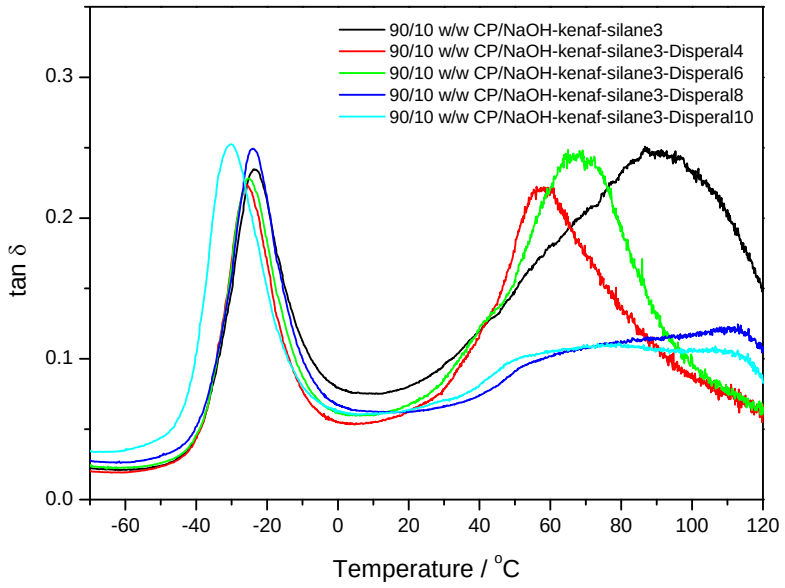

Figure 4.18 Damping factor (tan δ) as function of temperature of CP/NaOH-kenaf-silane3, and the CP/NaOH-kenaf-silane3-Disperal composites

4.6 Tensile testing

The tensile properties of neat CP and its natural fibre composites are shown in Figures 4.19 to 4.21 as function of silane and Disperal contents, and the values for Young's modulus, as well as stress and elongation at break, are summarized in Table 4.5. The stress-strain curves of all the investigated samples are shown in Appendix A.

The CP/kenaf and CP/NaOH-kenaf composites exhibit higher Young's modulus values, but lower stress and elongation at break values, than neat CP. The Young's modulus values are higher, because the introduction of fibre, whether modified or not, increases the stiffness of a polymer [24]. Fibres are well known for their rigidity and large strength. However, the NaOH treatment of the fibre in the CP/NaOH-kenaf composite gave rise to a higher elongation at break and Young's modulus than the CP/kenaf composite. This is the result of improved surface interaction between the fibre and the matrix because of mechanical interlocking brought about by an increase in surface roughness of the fibre. Similar observations were made in the investigation of the development of biocomposites with improved mechanical properties by Lee *et al.* [24]. The tensile strength and modulus of the alkali treated jute biocomposites were better than those of the untreated jute/solanyl biocomposites. It was explained as better stress transfer from the matrix to the alkali treated reinforcing fibrous filler. Other investigations on NaOH treated fibre have shown improved tensile strength, tensile modulus and elongation at break [25-27].

Figure 4.19 shows the Young's modulus values for silane and Disperal treated composites modified at different concentrations. The Young's modulus increases with increasing silane content for the silane treated composites. This indicates that the ductility of the composites is decreased while the stiffness of the composites is increased. This is attributed to the better interaction between the treated fibre and the matrix as a result of silane initiated crosslinking/grafting. Therefore, chain movement is restricted during deformation and results in stiff composites. The Disperal containing composites show irregular changes in the Young's modulus values, and no trend, so that nothing can be concluded from these results.

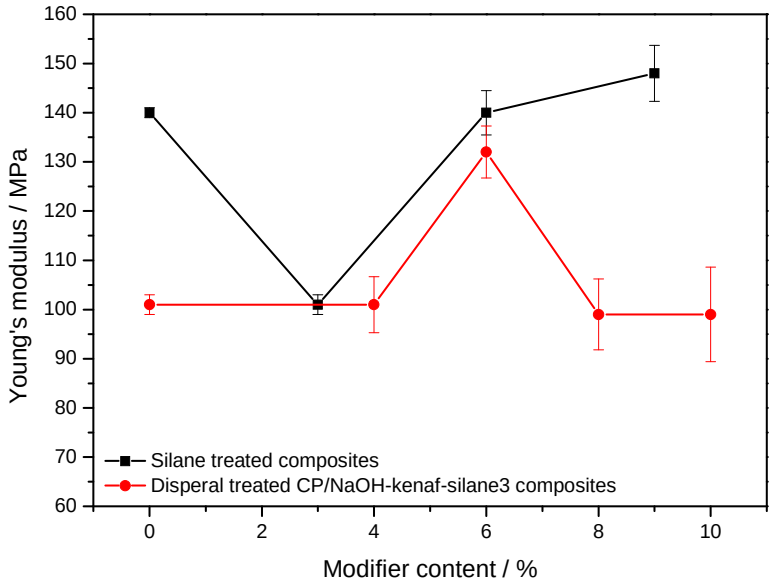

Figure 4.19 Young's modulus for silane and Disperal treated composites

Table 4.5 Summary of the tensile results for all the investigated samples

Samples	σ_b / MPa	ε_b / %	E / MPa
CP	10.5 ± 0.2	444	58.5 ± 1.7
CP/kenaf	6.6 ± 0.3	12.0 ± 0.3	99.0 ± 1.4
CP/NaOH-kenaf	6.8 ± 0.1	27.6 ± 1.7	140 ± 1
CP/NaOH-kenaf-silane3	6.6 ± 0.2	26.2 ± 1.0	101 ± 2
CP/NaOH-kenaf-silane6	6.3 ± 0.2	16.8 ± 0.3	148 ± 3
CP/NaOH-kenaf-silane9	6.5 ± 0.4	17.5 ± 1.5	140 ± 5
CP/NaOH-kenaf-silane3-Disperal4	6.1 ± 0.2	25.6 ± 5.7	101 ± 2
CP/NaOH-kenaf-silane3-Disperal6	7.4 ± 0.3	39.8 ± 0.8	132 ± 3
CP/NaOH-kenaf-silane3-Disperal8	6.6 ± 0.7	35.8 ± 4.0	99.0 ± 5.7
CP/NaOH-kenaf-silane3-Disperal10	6.8 ± 0.3	35.5 ± 4.7	99.0 ± 9.6

ε_y ,σ_y, ε_b, σ_b and E are elongation at yield, yield stress, elongation at break, stress at break, Young's modulus of elasticity

Figure 4.20 and Table 4.5 shows the stress at break of silane and Disperal treated composites. All the composites have stress at break values lower than that of neat CP, but there was no change in stress at break as a result of any of the treatments.

The elongation at break decreases with increasing silane content (Figure 4.21). The crosslinking/grafting restricts chain mobility, giving rise to lower elongation at break values. The Disperal treated composites show a slight increase in elongation at break. This indicates that the presence of Disperal plasticizes the CP matrix, which gives rise to increasing chain mobility of the polymer chains [23].

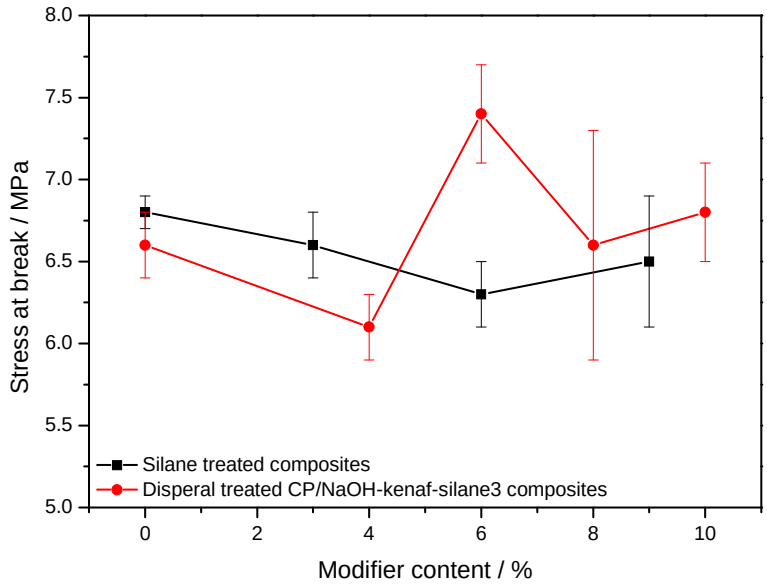

Figure 4.20 Stress at break for silane and Disperal treated composites

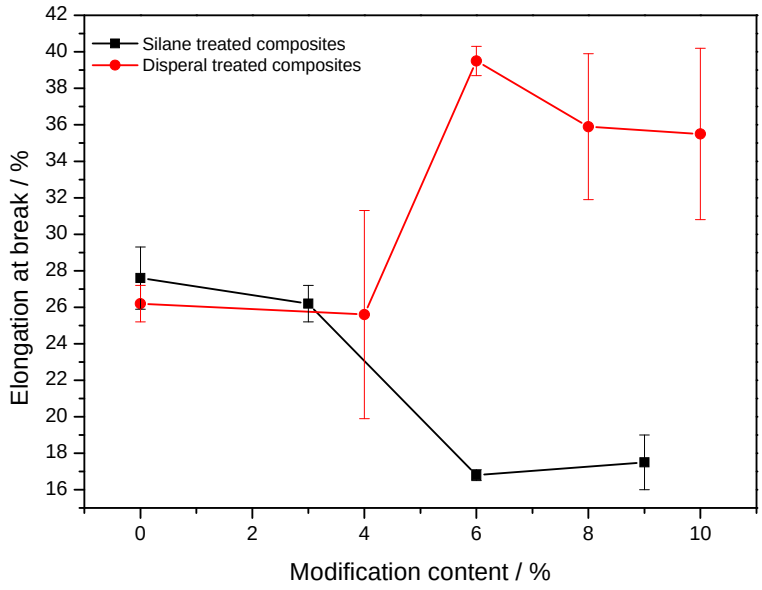

Figure 4.21 Elongation at break for silane and Disperal treated composites

4.7 Biodegradability tests

The biodegradability results for all the composites are shown in Figures 4.22 and 4.23, and summarized in Table 4.6. The weight loss (w_{loss} / %) was calculated using Equation 4.2.

$$w_{loss} = \frac{w_{initial} - w_{final}}{w_{final}} \times 100\ \% \qquad (4.2)$$

where $w_{initial}$ and w_{final} are the weights of the samples measured before and after exposing them to the environment for the indicated periods.

Figure 4.22 comparatively shows the weight loss of different composites, with and without silane treatment, as a function of exposure time. The kenaf reinforced composites seem to exhibit higher weight loss than the neat CP. Furthermore, the weight loss slightly increases with increasing time of exposure to the environment for all the specimens. There is no significant difference in the weight loss of CP and all the investigated composites up to 20 days. This may be due to fibre surfaces that are unexposed and covered by CP. After 20 days

the composites seem to degrade faster than the pure CP, but above 40 days all the samples seem to be equally degraded. However, the reported weight loss percentages are very small for all the samples, so statistically there are no real differences between the different samples.

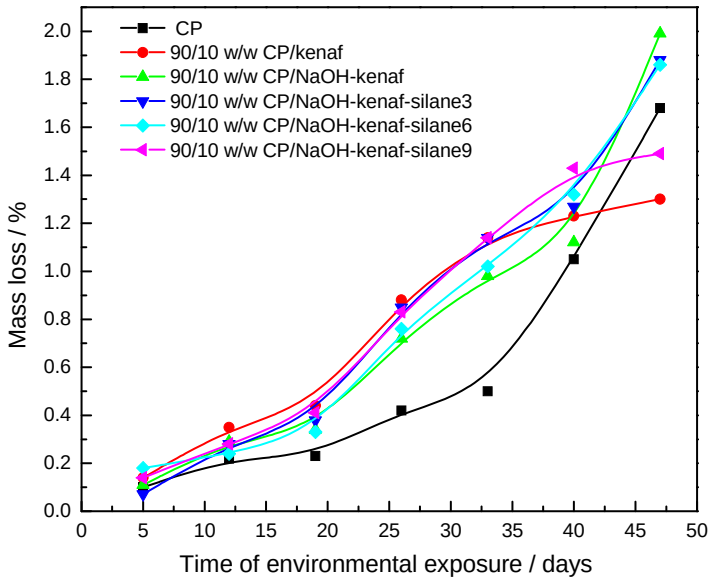

Figure 4.22 Biodegradability of silane treated composites

The biodegradation analyses was supposed to be performed on a number of samples per composition in order to obtain statistically relevant average values with standard deviations, and the tests should have been performed over longer periods of time. However, this could not be achieved due to insufficient material and due to limited time to do the tests. According to literature the effects of degradation were observably attained only after longer periods of burial or environmental exposure [28-30].

Figure 4.23 shows the influence of the presence and content of Disperal on the degradation behaviour of the CP/NaOH-kenaf-silane3 composites. There were no significant differences in the weight loss values of the different composites, and no trend was observed. As mentioned above, the analyses were not done on a statistically acceptable number of samples, and it is therefore assumed that Disperal had very little influence on the biodegradation of these composites.

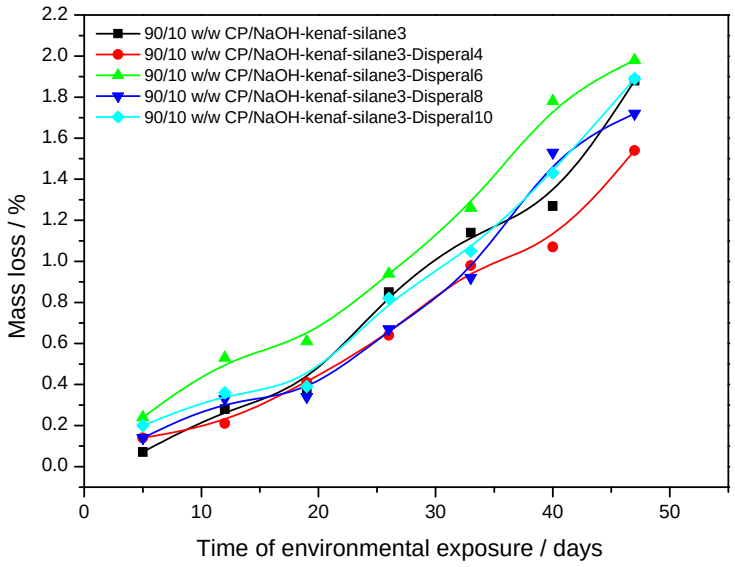

Figure 4.23 Biodegradability of Disperal treated composites

Table 4.6 Percentage mass loss of copolyester/kenaf fibre composites after environmental exposure for the indicated numbers of days

Samples	Day 5	Day 12	Day 19	Day 26	Day 33	Day 40	Day 47
CP	0.10	0.22	0.23	0.42	0.50	1.05	1.68
CP/kenaf	0.14	0.35	0.44	0.88	1.14	1.23	1.30
CP/NaOH-kenaf	0.11	0.29	0.34	0.72	0.98	1.12	1.99
CP/NaOH-kenaf-silane3	0.07	0.28	0.38	0.85	1.14	1.27	1.88
CP/NaOH-kenaf-silane6	0.18	0.24	0.33	0.76	1.02	1.32	1.86
CP/NaOH-kenaf-silane9	0.14	0.28	0.41	0.83	1.14	1.43	1.47
CP/NaOH-kenaf-silane3-Disperal4	0.14	0.21	0.41	0.64	0.98	1.07	1.54
CP/NaOH-kenaf-silane3-Disperal6	0.24	0.53	0.61	0.94	1.26	1.78	1.98
CP/NaOH-kenaf-silane3-Disperal8	0.14	0.33	0.34	0.67	0.92	1.53	1.72
CP/NaOH-kenaf-silane3-Disperal10	0.20	0.36	0.39	0.82	1.05	1.43	1.89

4.8 Gel content

The gel content results for the silane and Disperal treated composites are shown in Figure 4.24 and summarized in Table 4.7. The gel content was determined using the following equations.

$$W_{extracted} = W_{(sample+mesh)be} - W_{(sample+mesh)ae} \quad (4.3)$$

$$W_{polymer} = W_{sample} \times 0.9 \quad (4.4)$$

$$\% \text{ Extraction} = \frac{W_{extracted}}{W_{polymer}} \times 100\% \quad (4.5)$$

$$\% \text{ Gel} = 100 - \% \text{ Extraction} \quad (4.6)$$

where $w_{extracted}$ is the extracted weight, w_{sample} is the weight of the composite, $w_{(sample+mesh)be}$ and $w_{(sample+mesh)ea}$ are the weight of the composite and the mesh before and after extraction, and $w_{polymer}$ is the weight of polymer without fibre.

The results obtained show a decrease in the gel content as the amount of treatment is increased for both silane and Disperal treated composites. However, the silane treated composites in the absence of Disperal show higher gel content values, indicating more effective crosslinking/grafting. The gel content of these samples remained fairly constant within experimental error with increasing silane content. This indicates that higher silane contents did not really improve the crosslinking/grafting in these composites. This is in line with the DSC results that showed almost constant melting enthalpy values with increasing silane content. However, the Disperal treated composites show a significant decrease in the gel content with increasing Disperal content. The decrease in the gel content for Disperal composites might have been due to the interaction of silane with Disperal, which might have influenced the crosslinking/grafting efficiency of the silane. The FTIR results (section 4.2) showed vibrational peaks related to Al—O—Si–, that were taken as proof of an interaction/reaction between $(CH_3O)_3SiCH_2$ in silane and Al–OH in Disperal.

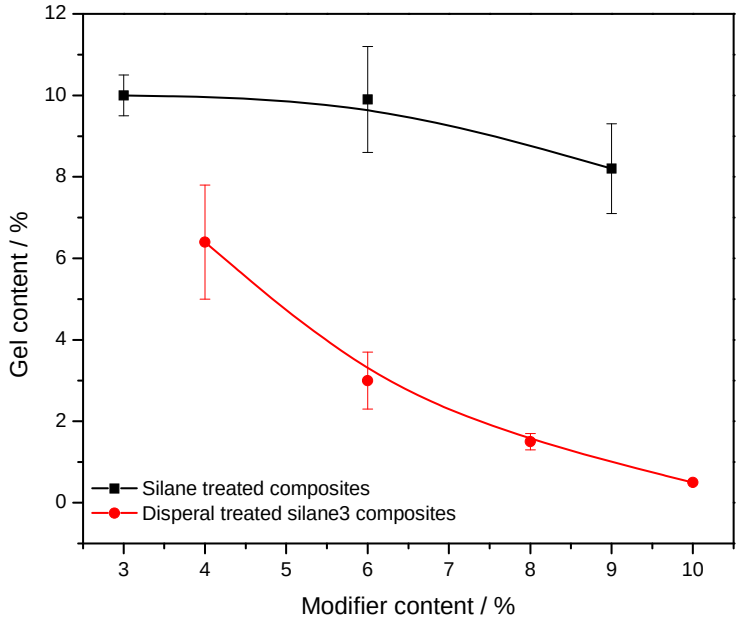

Figure 4.24 Gel content for silane and Disperal treated composites

Table 4.7 Gel contents for all the composite samples

Samples w/w	Gel content / %
90/10 CP/NaOH-kenaf-silane3	10.0 ± 0.5
90/10 CP/NaOH-kenaf-silane6	9.9 ± 1.3
90/10 CP/NaOH-kenaf-silane9	8.2 ± 1.1
90/10 CP/NaOH-kenaf-silane3-Disperal4	6.4 ± 0.4
90/10 CP/NaOH-kenaf-silane3-Disperal6	3.0 ± 0.7
90/10 CP/NaOH-kenaf-silane3-Disperal8	1.5 ± 0.2
90/10 CP/NaOH-kenaf-silane3-Disperal10	0.5 ± 0.0

4.9 References

1. W. Liu, A.K. Mohanty, P. Askeland, L.T. Drzal, M. Misra. Influence of fibre surface treatment on properties of Indian grass fiber reinforced soy protein based biocomposites. Polymer 2004:7589-7596.
   DOI: 10.1016/j.polymer.2004.09.009
2. N.E. Marcovich, M.A. Villar. Thermal and mechanical characterization of linear low-density polyethylene/wood flour composites. Journal of Applied Polymer Science 2003; 90:2775-2784.
3. P. Antich, A. Vázquez, I. Mondragon, C. Bernal. Mechanical behavior of high impact polystyrene reinforced with short sisal fibers. Composites Part A 2006; 37:139-150.
   DOI: 10.1016/j.compositesa.2004.12.002
4. V. Tserki, P. Matzionos, N.E. Zafeiropoulos, C. Panayiotou. Development of biodegradable composites with treated and compatibilized lignocellulosic fibers. Journal of Applied Polymer Science 2006; 100:4703-4710.
5. L.M. Arzondo, C.J. Pérez, J.M. Carella. Injection molding of long sisal fiber-reinforced polypropylene: Effects of compatibilizer concentration and viscosity on the fiber adhesion and thermal degradation. Polymer Engineering and Science 2005; 45: 613-621.
   DOI: 10.1002/pen.20299
6. A.K. Mohanty, M. Misra, G. Hinrichsen. Biofibres, biodegradable polymers and biocomposites: An overview. Macromolecular Materials and Engineering 2000; 276/277:1-24.
7. X. Li, L.G. Tabil, S. Panigrahi. Chemical treatments of natural fibre for use in natural fibre-reinforced composites. Journal of Polymers and the Environment 2007; 15:25-33.
   DOI: 10.1007/s10924-006-0042-3
8. Y. Habibi, W.K. El-Zawawy, M.M. Ibrahim, A. Dufresne. Processing and characterization of reinforced polyethylene composites made with lignocellulosic fibers from Egyptian agro-industrial residues. Composites Science and Technology 2008; 68:1877-1885.
   DOI: 10.1016/j.compscitech.2008.01.008
9. H.D. Rozman, B.K. Kon, A. Abusamah, R.N. Kumar, Z.A. Mohd. Ishak. Rubberwood-high-density polyethylene composites: Effect of filler size and coupling agents on mechanical properties. Journal of Applied Polymer Science 1998; 69:1993-2004.

10. H.D. Rozman, K.W. Tan, R.N. Kumar, A. Abubakar, Z.A. Mohd. Ishak, H. Ismail. The effect of lignin as a compatibilizer on the physical properties of coconut fiber-polypropylene composites. European Polymer Journal 2000; 36:1483-1494.
11. L.A. Pothan, J. George, S. Thomas. Effect of fiber surface treatment on the fiber-matrix interaction in banana fiber reinforced polyester composites. Composite Interfaces 2002; 9:335-353.
12. C.U. Maheswari, B.R. Guduri, A.V. Rajulu. Properties of lignocellulose tamarind fruit fibers. Journal of Applied Polymer Science 2008; 110:1986-1989.
DOI: 10.1002/app.27915
13. W.L. Lai, M. Mariatti, S.J. Mohamad. The properties of woven kenaf and betel palm (*Areca catechu*) reinforced unsaturated polyester composites. Polymer-Plastics Technology and Engineering 2008; 47:1193-1199.
DOI: 10.1080/03602550802392035
14. L. Liu, J. Yu, L. Cheng, X. Yang. Biodegradability of poly(butylene succinate) (PBS) composite reinforced with jute fibre. Polymer Degradation and Stability 2009; 94:90-94.
15. J.M. He, Y.D. Huang. Effect of silane-coupling agents on interfacial properties of CF/PI composites. Journal of Applied Polymer Science 2007; 106:2231-2237.
DOI: 10.1002/app.26875
16. S.C. Shen, Q. Chen, P.S. Chow, G.H. Tan, X.T. Zeng, Z. Wang, R.B.H. Tan. Steam-assisted solid wet-gel synthesis of high-quality nanorods of boehmite and alumina. Journal of Physical Chemistry 2007; 111:700-707.
DOI: 10.1021/jp065767d
17. S. Ram. Infrared spectral study of molecular vibrations in amorphous, nanocrystalline and $AlO(OH)\cdot\alpha\ H_2O$ bulk crystals. Infrared Physics and Technology 2001; 42:547-560.
18. Q. Chen, C. Udomsangpetch, S.C. Shen, Y.C. Liu, Z. Chen, X.T. Zeng. The effect of AlOOH boehmite nanorods on mechanical property of hybrid composite coatings. Thin Solid Films 2009; 517:4871-4874.
DOI: 10.1016/j.tsf.2009.03.097
19. W. Brostow, T. Datashvili. Chemical modification and characterization of boehmite particles. Chemistry and Chemical Technology 2008; 2:27-31.
20. H. Sharifah, M.P. Ansell. The effect of alkalization and fibre alignment on the mechanical and thermal properties of kenaf and hemp bast fibre composites: Part 1-Polyester resin matrix. Composites Science and Technology 2004; 64:1219-1230.
DOI: 10.1016/j.compscitech.2003.10.001

21. A.K. Saha, S. Das, D. Bhatta, B.C. Mitra. Study of jute fiber reinforced polyester composites by dynamic mechanical analysis. Journal of Applied Polymer Science 1999; 71:1505-1513.
22. K.C. Manikandan Nair, S. Thomas, G. Groeninckx. Thermal and dynamic mechanical analysis of polystyrene composites reinforced with short sisal fibres. Composites Science and Technology 2001; 61:2519-2529.
23. A. Dufresne, M.N. Belgacem. Cellulose-reinforced composites: Fro micro-to nanoscale. Polímeros: Ciência e Tecnologia 2010; 20:1-10.
DOI: 10.4322/polimeros.2010.01.001
24. M.W. Lee, S.Y. Ho, K.P. Lim, T.T. Ng, Y.K. Juay. Development of biocomposites with improved mechanical properties. SIMTech Technical Reports 2008; 9:115-118.
25. I.S. Aji, S.M. Sapuari, E.S. Zainudin, K. Abdan. Kenaf fibres as reinforcement for polymeric composites. International Journal of Mechanical and Materials Engineering 2009; 4: 239-248.
26. A.M. Edeerozey, H.M. Akil, A.B. Azar, M.I.Z. Ariffin. Chemical modification of kenaf fibers. Materials Letters 2007; 61:2023-2025.
DOI: 10.1016/j.matlet.2006.08.006
27. W.W.M Hazira, An-Sariumiah, A.M. Moh'd, I. Norsaadah. Treatment of kenaf for LDPE-kenaf composites. Proceedings of the Third Technical Review Meeting on the National Kenaf Research Project. Kota Bharu, Kelantan 25-26 May 2004.
28. N. Teramoto, K. Urata, K. Ozawa, M. Shibata. Biodegradation of aliphatic polyester composites reinforced by abaca fiber. Polymer Degradation and Stability 2004; 86:401-409.
DOI: 10.1016/j.polymdegradstab.2004.04.026
29. L. Liu, J. Yu, L. Cheng, X. Yang. Biodegradability of poly(butylene succinate) (PBS) composite reinforced with jute fibre. Polymer Degradation and Stability 2009; 94:90-94.
DOI: 10.1016/j.polymdegradstab.2008.10.013
30. T. Behjat, A.R. Russly, C.A. Luqman, C.A. Yus, I. Nor Azowa. Effects on the biodegradability studies of kenaf cellulose-polyethylene composites. International Food Research Journal 2009; 16:243-247.

CHAPTER FIVE

CONCLUSIONS

The purpose of this study was to investigate the thermal and reinforcement properties of modified kenaf fibre introduced into a copolyester (CP) biomatrix (aliphatic-aromatic copolyester – trade-name Ecoflex). This was achieved by comparing the properties of CP and CP/kenaf (untreated) with composites where the fibre was treated with sodium hydroxide, silane and Disperal nanoparticles.

The reinforcement of the CP matrix with unmodified kenaf fibre showed poor fibre-matrix interaction as seen by SEM. However, the presence of kenaf fibre improved the stiffness of the CP matrix. The storage and Young's modulus of the CP/kenaf composite was higher than that of CP as a result of the presence of the stiffer fibre. The presence of kenaf in the CP/kenaf composite did not significantly change the melting temperature or melting enthalpy of CP, which shows that the crystallization of the polymer was not influenced by the presence of the untreated fibre. The thermal stability of the CP was reduced by the introduction of unmodified fibre. The CP/kenaf showed a higher biodegradability than CP, but the mass loss percentages were very small for all the samples, so statistically there was very little difference between the different samples.

The CP/NaOH-kenaf composite showed better tensile properties than the CP/kenaf composite. It had a higher Young's modulus and larger elongation at break than the CP/kenaf composite. The tensile results are in line with the DMA results where a high modulus was also observed. The improved fibre-matrix adhesion as a result of the fibre treatment with NaOH, as seen by SEM, may have contributed to the increased modulus of the CP/NaOH-kenaf composite. The NaOH treated composite showed evidence of fibre-matrix interaction which was not visible for the CP/kenaf composite. The NaOH treated fibres also did not significantly influence the melting temperature or melting enthalpy of CP. The observed enthalpy had the same order of magnitude than the calculated enthalpy, indicating that the crystallization of the polymer was not influenced by the presence of NaOH-kenaf. The CP/NaOH-kenaf composite showed better thermal stability than the CP/kenaf composite. This was probably because the alkali treatment brought about an increased surface roughness in the fibre which resulted in better mechanical interlocking between the filler and the matrix. The improved surface roughness

was implied by the FTIR results, which showed the disappearance of vibrational peaks related to the functional groups of lignin and hemicellulose. The biodegradability of the CP/NaOH-kenaf was very similar to that of CP/kenaf.

The silane modified composites showed improved fibre-matrix interaction due to grafting, which was seen in SEM and in FTIR that showed the presence of siloxane functional groups. However, the silane grafting in the CP/NaOH-kenaf composite caused a slight shift in the melting peaks to higher temperatures, but the melting and crystallization enthalpies were too scattered to draw any firm conclusions from the DSC results. The silane treated CP/NaOH-kenaf composites showed lower thermal stabilities than the CP/NaOH-kenaf composite. Silane treatment resulted in a reduction of the storage modulus of the composites. The tensile results of the silane treated composites also showed a reduced modulus value, but the stress and strain at break were of the same order of magnitude as those of CP/NaOH-kenaf. The biodegradability results did not differ significantly from that of CP/NaOH-kenaf, and statistically there were no real differences between the different samples. The gel content results of the silane treated composites showed the presence crosslinking/grafting in the samples.

The introduction of Disperal nano-powder into the CP/NaOH-kenaf-silane3 composite showed good adhesion between the fibre and the matrix as seen by SEM, and the FTIR results showed some silane-Disperal interaction. The decomposition temperatures of these composites were higher than that of CP/NaOH-kenaf-silane3. However, the composites with Disperal showed some plasticization of the composite, which was clear from the DMA and tensile modulus values. The thermal property values from the DSC were too scattered to draw any significant conclusions. The presence of Disperal generally had very little influence on the properties of the composites, except for some improvement in the thermal stability.

In summary it can be said that the best balance of properties were observed in the case of CP/NaOH-kenaf. This composite showed improved thermal, thermomechanical, and mechanical properties. The introduction of alkali treatment caused increased surface roughness in the fibre, which resulted in mechanical interlocking between the filler and the matrix, while silane treatment slightly reduced the properties and the presence of Disperal had almost no influence on the properties.

ACKNOWLEDGEMENTS

- Above all, special thanks are extended to the **Lord Jesus Christ** my Saviour for providing me with the strength and heart to stand throughout this project. For the knowledge, wisdom and understanding that He grants to us when we ask in His name. "*I can do all things through Christ who strengthens me*" Phillippians 4:13

- My gratitude and appreciation to my supervisor **Prof. Adriaan Stephanus Luyt**, for his consistent supervision, guidance, encouragement and patience during all stages of this project. His overly enthusiasm and integral view on research and his mission for providing 'only high-quality work and not less', has made a deep impression on me.

- I am also grateful to my co-supervisor **Dr. Babu R. Guduri**, for following the progress and providing technical guidance and valuable contributions throughout the research program.

- I acknowledge the financial support from NRF and the University of the Free State. Special thanks to CSIR (MSM, Polymers and Composites group) for their support that was provided to me during my internship programme and research work. I acknowledge the following people that I worked with closely at the CSIR: Selina Makhele, Philemon Matabola, Dioce Moyo and Nontsikelelo Dumakude, for their support, guidance and encouragement through tough times during this project.

- Special thank to Jeremia Shale Sefadi, who has been more a brother than a friend. For his support, advice, encouragement and most for being there in times of troubles through the course of this project.

- I am grateful to the faculty, staff and colleagues in the Department of Natural and Agricultural sciences for their assistance in every aspect of my project. To the entire polymer research team (PhD, M.Sc and Honours). Special thanks to Puseletso Mofokeng and Essa Ahmad, for their support throughout this project. Also to Mfiso Mngomezulu, Tshwafo Motaung, and Samsom Mohomane.

- To my Family: Matlholi Jerminah Mokhothu (mother), Tshepiso Mokhothu (sister), Motlalepule Mokhothu (grandmother) and Steven Moremi (Uncle), for their support, wisdom and encouragement to further my studies. Special thank to Masene Mokhothu (Rakgadi), Abuti Thabo Moloi, for being my parents and accommodating me in their home since I started my postgraduate studies, for their love, support and encouragement towards my studies. To Tladi Mokhothu, Dr. Joyce Moloi, Bernard Motshoko, Peter Motshoko and Nkgono Masima (mama) for their day to day support. Special gratitude to Nathiseng Molaba and Bokamoso Elizabeth (Daughter), for being always excused among them for my M.Sc. degree studies, their patience, support and love. Special dedication to my Cousins: Tebogo Weer, and Mpho Mongale. "*Perseverance is the mother of success*"

- To Shield of Love ministry, for their every day prayers, love and support. May the Almighty God pour out blessings to each and every one of them and their families.

- I am also grateful to my many friends for their support, motivation towards my studies: Teboho Mofokeng, Ditaba Radebe, Khulekani Vilakazi, Paleho Lepota, Edward Sikhosana, Thabiso Skhosana, Tello Mokgoko, Sthembiso Khumalo, Karedi Motsau, Sidney Khuduga and Malefetsane Mokwatle. "Ayobaness Gents". Also to the friends I met in Port Elizabeth: Mothusi Mbole, Rhuang, Memory and Abigail.

APPENDIX

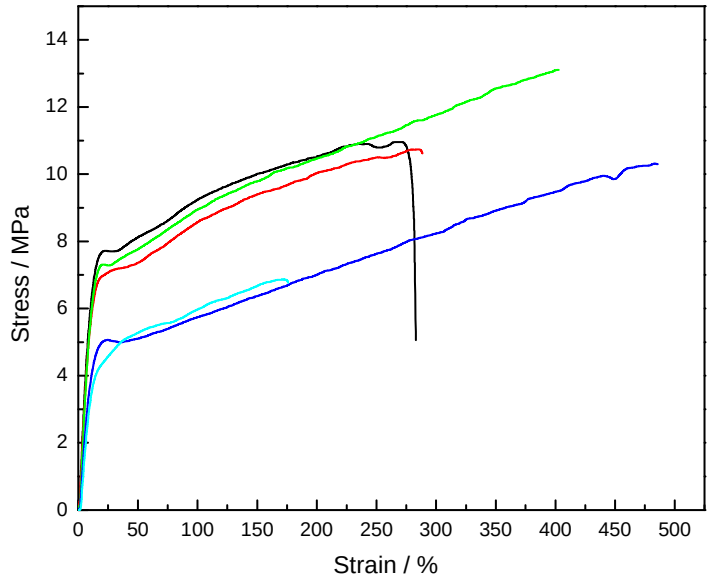

Figure A.1 Stress-strain curves for the copolyester

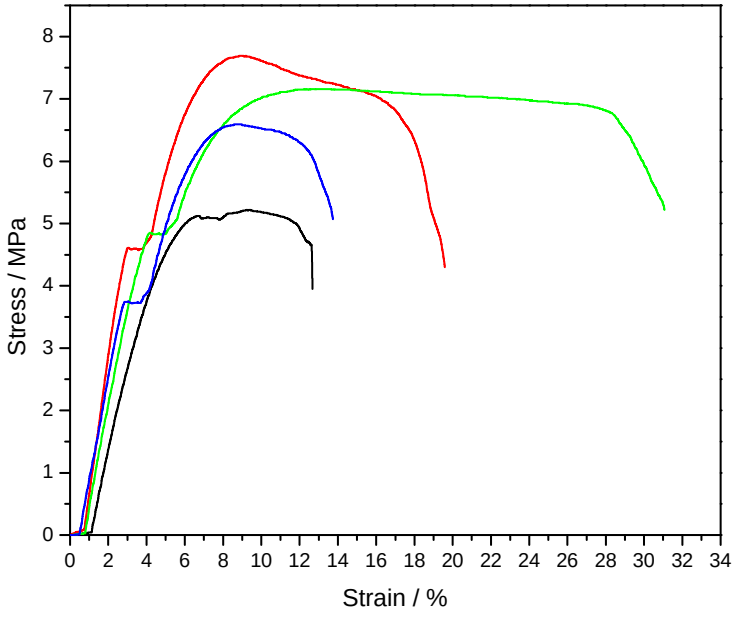

Figure A.2 Stress-strain curves for the 90/10 w/w CP/kenaf composite

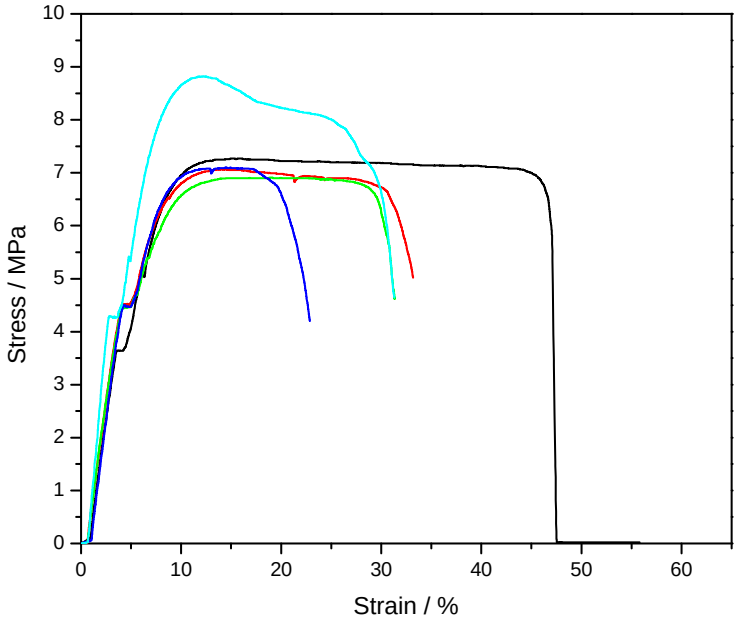

Figure A.3 Stress-strain curves for the 90/10 w/w CP/NaOH-kenaf composite

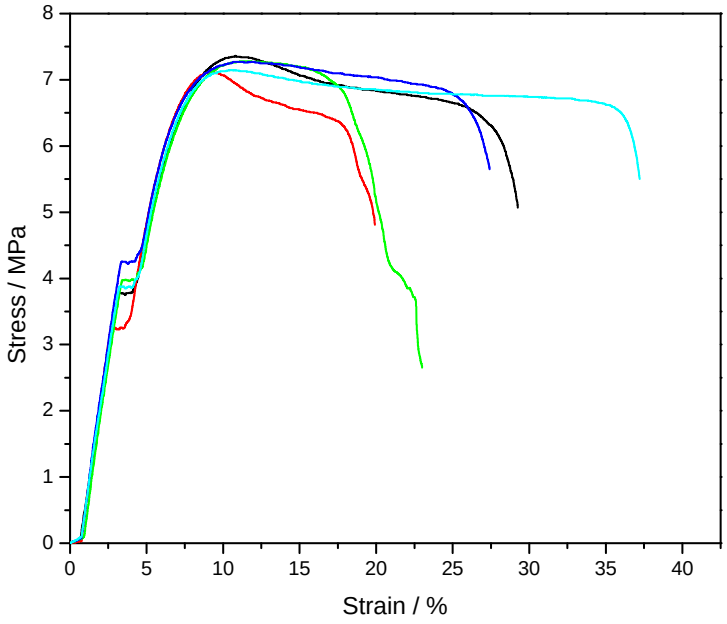

Figure A.4 Stress-strain curves for the 90/10 w/w CP/NaOH-kenaf-silane3 composite

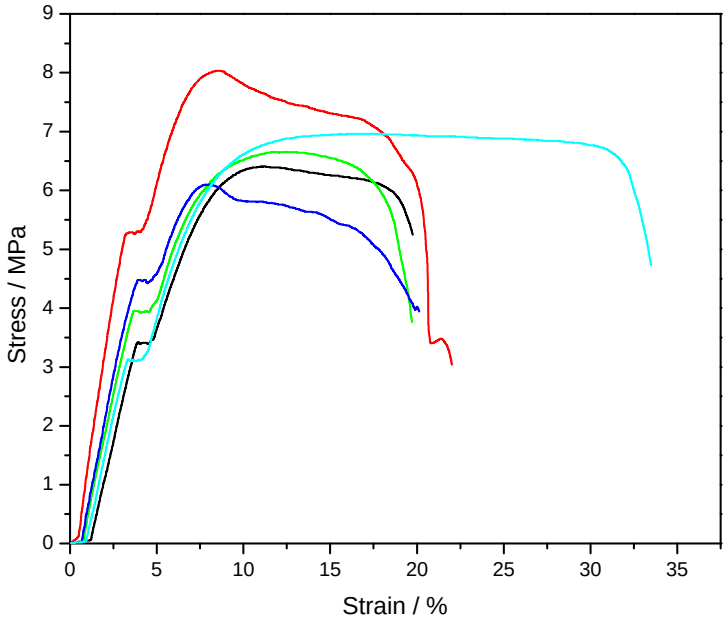

Figure A.5 Stress-strain curves for the 90/10 w/w CP/NaOH-kenaf-silane6 composite

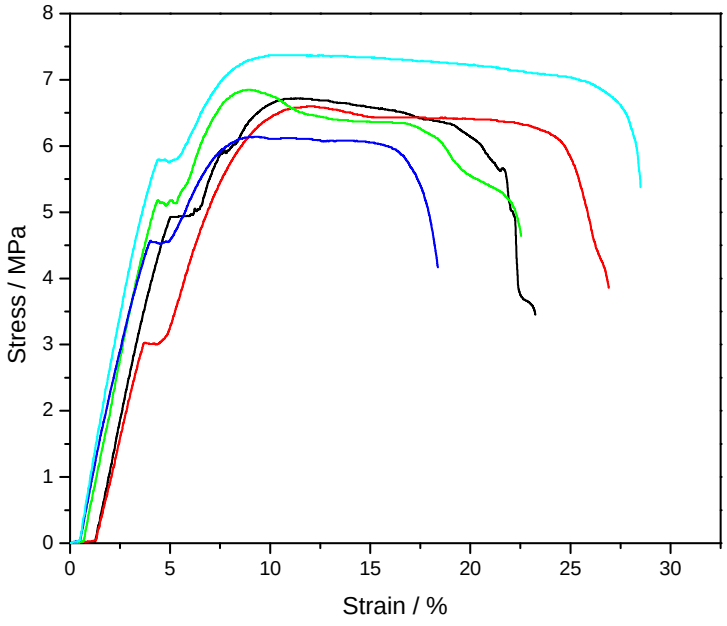

Figure A.6 Stress-strain curves for the 90/10 w/w CP/NaOH-kenaf-silane9 composite

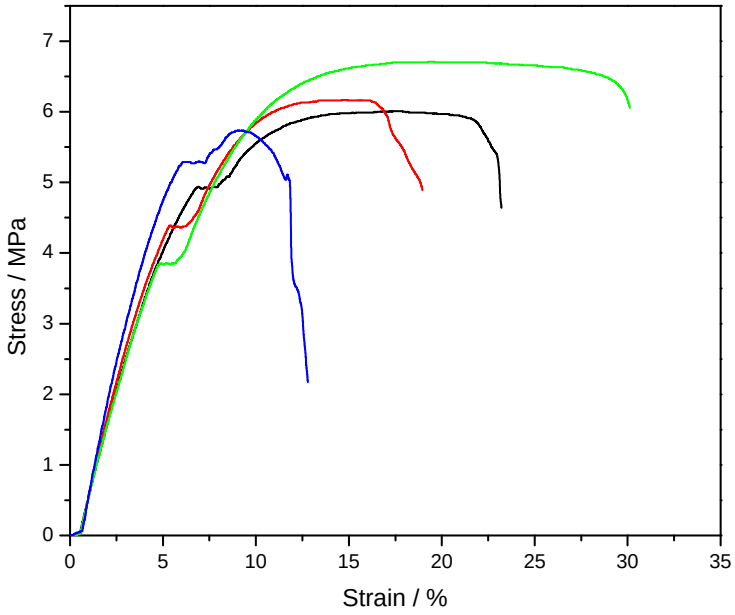

Figure A.7 Stress-strain curves for the 90/10 w/w CP/NaOH-kenaf-silane3-Disperal4 composite

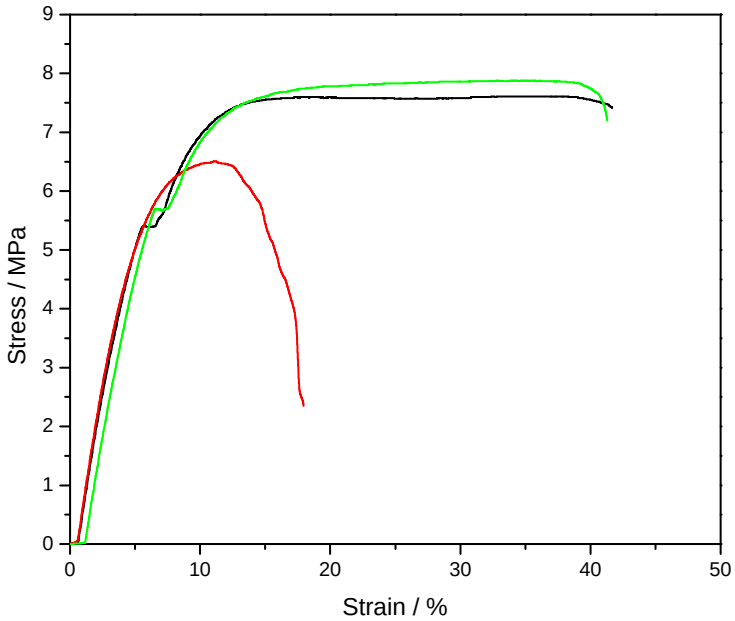

Figure A.8 Stress-strain curves for the 90/10 w/w CP/NaOH-kenaf-silane3-Disperal6 composite

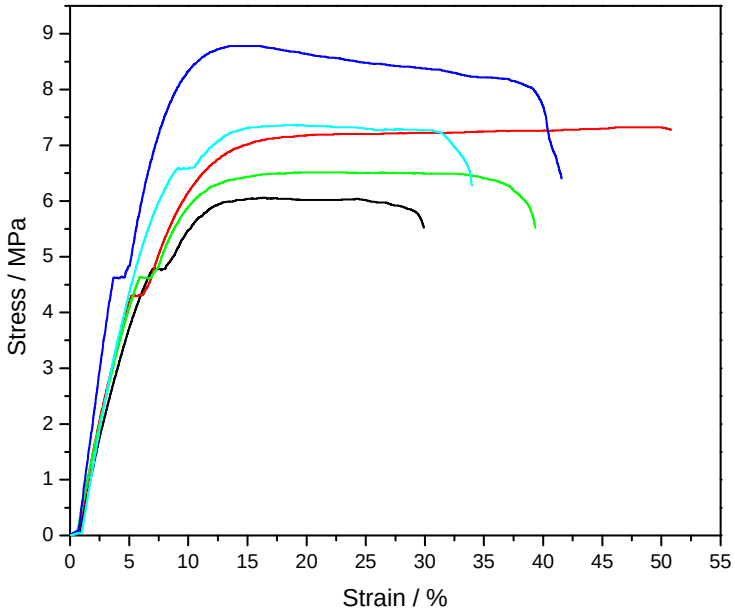

Figure A.9 Stress-strain curves for CP/NaOH-kenaf-silane3-Disperal8 composite

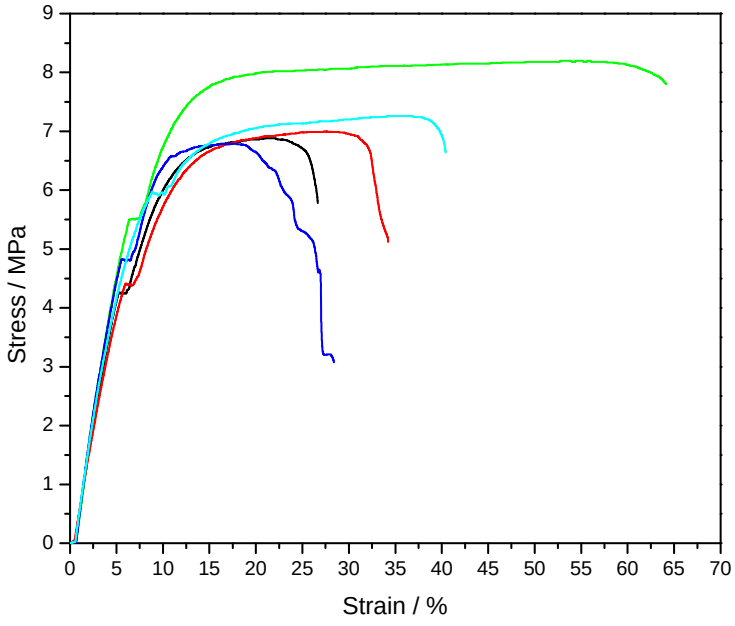

Figure A.10 Stress-strain curves for the 90/10 w/w CP/NaOH-kenaf-silane3-Disperal10 composite